LATE CRETACEOUS THROUGH PALEOGENE RECONSTRUCTION OF PACIFIC DEEP-WATER CIRCULATION

A Thesis

by

JESSICA ANNA SCHUBERT

Submitted to the Office of Graduate Studies of
Texas A&M University
in partial fulfillment of the requirements for the degree of

MASTER OF SCIENCE

May 2012

Major Subject: Oceanography

Late Cretaceous through Paleogene Reconstruction of Pacific Deep-Water Circulation

LATE CRETACEOUS THROUGH PALEOGENE RECONSTRUCTION OF PACIFIC DEEP-WATER CIRCULATION

A Thesis

by

JESSICA ANNA SCHUBERT

Submitted to the Office of Graduate Studies of
Texas A&M University
in partial fulfillment of the requirements for the degree of

MASTER OF SCIENCE

Approved by:

Chair of Committee,	Deborah J. Thomas
Committee Members,	Mitchell W. Lyle
	Robert L. Korty
Head of Department,	Piers Chapman

May 2012

Major Subject: Oceanography

ABSTRACT

Late Cretaceous through Paleogene Reconstruction of Pacific Deep-Water Circulation

(May 2012)

Jessica Anna Schubert, B.S., The University of Texas at Austin

Chair of Advisory Committee: Dr. Deborah J. Thomas

A growing body of Nd isotope data derived from fish debris and Fe-Mn crusts suggests that the Pacific was characterized by deep-water mass formation in both the North and South Pacific during the Early Paleogene. However, the South Pacific source has not been identified to date. Here we present new fossil fish debris neodymium isotope data from the South Pacific and southern tropical Pacific Ocean Drilling Program and Deep Sea Drilling Project Sites 323, 463, 596, 865 and 869 (paleowater depths spanning 1500 to 5000m) to reconstruct the water mass composition over the time interval ~80 to ~24 Ma.

The data indicate a relatively unradiogenic South Pacific water mass composition, and the composition of Nd increases with distance northward. The new tropical Pacific data are consistent with existing records from that region. Analyses of detrital sediment Nd isotopic composition, combined with the dissolved Nd composition recorded by fish debris, suggests that the South Pacific water mass convected in the Pacific sector of the Southern Ocean. We designate this water mass South Pacific Deep Water (SPDW). The Nd isotopic composition of SPDW is more radiogenic than initially hypothesized and the relatively small increase in isotopic composition (from ~-6 to ~-4) during the transit from the Southern Ocean to the tropical Pacific suggests a faster rate of overturning circulation during the greenhouse climate interval than previously thought.

For My Dad

ACKNOWLEDGEMENTS

First I would personally like to thank my advisor, Debbie Thomas, who has guided me throughout my journey and has supported me in both good times and in bad. I sincerely appreciate you pushing me in my graduate program. Also, I would like to thank my committee members, Rob Korty and Mitch Lyle, for their valuable guidance and support of this research. I would like to also acknowledge my gratitude to the National Science Foundation, NSF-ATM award 0927769 and NSF S-STEM award 0806926 for funding my research.

A special thank you also goes to Stella Woodard, Dan Murphy and Tashina Chapman Jordon, for their generous guidance, teaching, and technical support in the radiogenic clean lab. I also want to extend a thank you to my friends and colleagues and the Department of Oceanography faculty and staff for all my good memories at Texas A&M University.

Finally, thanks to my mom for her encouragement, love and support throughout my entire education. And to John Alex Parker for always being there at the right moment with continuous support as a true Aggie.

NOMENCLATURE

Elements

Co	Cobalt
Fe	Iron
Mn	Manganese
Nd	Neodymium
REE	Rare Earth Element
Re	Rhenium
Sm	Samarium
Sr	Strontium

Units

Ma	Million years ago
mbsf	meters below sea floor
Myr	Million years
ppt	parts per thousand
μm	micrometer
μl	microliter

Water Masses

AABW	Antarctic Bottom Water
AAIW	Antarctic Intermediate Water
CDW	Circumpolar Deep Water
NADW	North Atlantic Deep Water
NPIW	North Pacific Intermediate Water
NPDW	North Pacific Deep Water
SPDW	South Pacific Deep Water
WSDW	Warm Saline Deep Waters

Other

CC	Core Catcher
CCD	Carbonate compensation depth
CHUR	Chondritic Uniform Reservoir
DSDP	Deep Sea Drilling Project
FO	First Occurrence
ITCZ	Intertropical Convergence Zone
LO	Last Occurrence
MOC	Meridional Overturning Circulation
ODP	Ocean Drilling Program
SST	Sea surface temperature
TIMS	Thermal Ionization Mass Spectrometer

TABLE OF CONTENTS

Page

LIST OF FIGURES

LIST OF TABLES

1. INTRODUCTION

The early Paleogene (~65-40 Ma) was a period of extreme global warmth characterized by diminished equator to pole thermal gradients, as well as diminished contrast between oceanic surface- and deep-water temperatures. Oxygen isotope records from Antarctic high latitudes indicate sea surface temperatures (SST) were ~11-15 °C, approximately 10°C warmer than the modern, for most of the early Paleogene (Stott et al., 1990; Zachos et al., 1994). Reconstructions of southwestern Pacific SSTs suggest temperatures of ~30°C during the Late Paleogene (Hollis et al., 2009). Estimates of tropical Pacific SSTs range from ~ 25-32°C during the early Eocene (Tripati et al., 2003). Deep-water temperatures during the early Paleogene were also ~10°C warmer than modern bottom waters (Zachos et al., 2001; 2008). Such warm deep-water temperatures suggest that both poles were largely free of significant permanent ice (Zachos et al., 2008). This overall pattern of warmth is consistent with higher levels of atmospheric CO_2 than present, and proxy data suggest that atmospheric CO_2 was higher than 1000ppm during this greenhouse period (Pearson and Palmer, 2000; Pagani et al., 2005).

Early Paleogene high latitude sea surface temperatures suggest higher heat transport from the tropics to the poles, however the existence of lower SST gradients from equator-to-pole as well as from surface to deep waters is at odds with enhanced poleward heat transport. Several modeling studies of the Paleogene reproduce close-to-modern or weaker values of ocean heat transport (Huber and Sloan, 2001; Najjar et al., 2002). However other models suggest diminished vertical thermal gradients may have

---

This thesis follows the style of *Paleoceanography*.

been associated with widespread mixing across a weaker thermocline (Lyle, 1997; Hay et al., 2005; Korty et al., 2008). The "paradox" of early Paleogene heat transport is still a subject of considerable debate and the first step in resolving this issue is a robust reconstruction of meridional overturning circulation (MOC).

The MOC is responsible for a significant component of global heat transport in the modern ocean. The present mode of MOC is characterized by deep-water formation at high latitudes in the North Atlantic and Southern Ocean. Several lines of evidence suggest that this Atlantic-dominated mode of convection likely did not operate during the early Paleogene. As discussed below, the early Paleogene was characterized by different continental and oceanic plate configurations. These differences in ocean basin geometry, combined with the different thermal structure described above, likely dictated a different pattern of MOC for the early Paleogene oceans.

A growing body of Nd isotope data suggests that a bipolar mode of MOC may have operated in the Pacific, as opposed to the Atlantic, during the early Cenozoic greenhouse (Thomas, 2004; Thomas et al., 2008; Hague et al., in review). The available data indicate the deep tropical Pacific was a mixing location of water masses that sank in both the Southern Ocean and North Pacific from ~65 to 45 Ma (Thomas, 2004), with little inter-basin exchange between the Pacific and Atlantic basins (Thomas et al., 2008). Most of the existing Pacific data are from the tropical to temperate North Pacific. Thus in order to better constrain the composition of waters presumed to have formed in the Southern Ocean we must look to sites located further south at the time. Here we present new fossil fish debris Nd data from the southern and tropical Pacific to test the hypothesis that one source of deep waters to the Pacific during the early Paleogene formed in the Pacific sector of the Southern Ocean.

2. BACKGROUND

2.1 *Modern Thermohaline Circulation*

Under modern conditions, deep-water formation occurs in the North Atlantic and Southern Ocean at high latitudes, with slow deep-water renewal in the North Pacific. Northern Atlantic deep waters are sourced from Nordic Seas and the Labrador Sea. Relatively higher surface salinity concentrations in the North Atlantic (~35 ppt (Levitus, 1982)) enable waters to become dense enough to sink once subjected to intense atmospheric cooling. Downwelling in the modern North Pacific is not significant because of lower surface salinities (~33 ppt (Levitus, 1982)) and a shallow Bering Strait sill limiting Arctic bottom waters to enter the North Pacific (Coachman et al., 1975). As a consequence, deep waters in the Pacific are much older than that of the Atlantic Ocean (Primeau, 2005).

The dominant water masses in the Pacific are the North Pacific Intermediate Water (NPIW) and Antarctic Bottom Water (AABW). NPIW found in the western North Pacific ranges in depths between 300 and 800 meters (You, 2003) and extends south to 15-20°N (Talley et al., 1995). The AAIW formed in the Southern portion of the Pacific ranges between 700 to 1400 meters, and extends northward under the equator (Talley et al., 2003). Deep water formed in the North Atlantic flows southward and mixes into and re-sinks as part of Antarctic Bottom Water (AABW) in the Southern Ocean. Portions of this water advect northward into the Antarctic Convergence and become subducted as part of Antarctic Intermediate Water (AAIW), which is redistributed into the Pacific Ocean as it flows northward and later comes into contact with NPIW.

2.2 *Paleogeographic Boundary Conditions*

Ocean circulation during the early Paleogene likely was constrained by the configuration of ocean basins and continents, which was different from the modern. The Pacific basin was larger proportionately than the Atlantic during the early Cenozoic. During the

Cenozoic, continental plate boundaries shifted significantly (Daly et al., 1989; Hall et al., 2002). Gondwana had broken up into separate Indian and Australia plates by the end of the Cretaceous. The northward movement of India resulted in a collision with the Asian continent by ~50 Ma (Hall et al., 2002), altering many Pacific plate interactions as a result of the collision, including the initiation of Pacific plate subduction in the westward direction along the Asian margin (Hall et al., 2002). These subduction events formed and maintained many of the volcanic island arcs in the Northern Pacific region throughout the early Cenozoic.

In the Southern Hemisphere, spreading rates after the rifting of Australia from Antarctica an earlier separation during the Cretaceous were extremely slow, leading to possible land connections through Tasmania into Antarctica (Hall, 2001). At 55 Ma, the Tasman Sea had not yet fully opened and continental fragments east of Australia were widely separated almost to their present-day positions (Hall, 2001, Stickley et al., 2006). In addition, the Western Antarctic margin was tectonically active. A spreading center in the eastern Amundsen Sea, off of western Antarctica, created sea floor spreading between the Pacific, Bellingshausen, Phoenix, and Antarctic plates starting ~76 Ma. Consequently, the Phoenix plate subducted under Antarctica throughout the Cenozoic (Eagles et al., 2004), contributing to arc volcanism in the region. The Phoenix plate was completely subducted by ~3.3Ma, and the margin changed to a passive setting (Eagles et al., 2004).

These changes in the tectonic configuration of ocean basins and landmasses impacted pathways of oceanic circulation over the early Paleogene. Major oceanic gateways, such as the Tasman Sea and Drake Passage were not open during this time (Frakes and Kemp, 1972, Lawver and Gahagan, 1998, 2003), thus circum-Antarctic circulation had not yet developed. Only shallow connections existed between the Arctic and Tethys Oceans (Stickley et al., 2004). Open seaways in Caribbean and Tethyan Sea potentially allowed for oceanic exchange at lower latitudes between the Atlantic and Pacific oceans.

Warm Saline Deep Waters (WSDW) are inferred to have formed in low latitude regions of net evaporative conditions during warm climatic intervals (Chamberlin, 1906; Brass et al., 1982). The eastern Tethys Sea likely was a region of high evaporation, and therefore a potential source of warm, saline waters to the intermediate and deep Pacific (e.g., Barron and Peterson, 1991). However, numerical models are unable to produce stable convection in the Tethys Sea region during the early Paleogene (Bice, 2001). More recent model simulations of circulation during past warm climate intervals suggest deep-water formation strong export of heat from low latitudes to the polar regions by ocean overturning (Hotinski and Toggweiler, 2003). Proxy data also yield conflicting results. Scher and Martin (2004) suggested that relatively low Nd isotope values recorded at ODP Site 689 (Maud Rise, Antarctic Ocean) derived from sinking in the Tethys Sea during the middle Eocene (Scher and Martin, 2004). In addition, work from the tropical Atlantic from ODP Leg 207 (Demerara Rise) suggests possible local convection of warm surface waters during the mid- to Late Cretaceous (Friedrich et al., 2008; MacLeod et al., 2008). But Thomas et al. (2003) suggested that deep waters formed in the Atlantic sector of the Southern Ocean and subsequent work revealed no contribution of Tethyan waters to the Cretaceous or Paleogene Pacific (e.g., Thomas et al., 2008; Murphy and Thomas, in revision).

2.3 *Neodymium Isotope Tracer of Water Mass Composition*

The isotopic composition of Neodymium (Nd), a light Rare Earth Element (REE), is a useful tracer of oceanic water masses. The nuclide ^{143}Nd is produced by the radioactive decay of ^{147}Samarium (Sm; half-life = 1.06 X 10^{11} yrs). Values of ^{143}Nd/^{144}Nd for the Earth follow a growth curve, resulting from the ^{147}Sm/^{144}Nd ratio of Chondritic Uniform Reservoir (CHUR). ^{143}Nd/^{144}Nd samples normalized to the bulk earth are expressed as ε_{Nd} where:

$$\varepsilon_{Nd} = (((^{143}Nd/^{144}Nd \text{ sample}/0.512638) \times 10{,}000) - 1$$

(DePaolo & Wasserburg, 1976). In ancient samples, a correction for age must be also taken in account for in situ production of ^{143}Nd from ^{147}Sm in the sample. The age corrected values are presented as $\varepsilon_{Nd}(t)$.

Rocks evolve different $^{143}Nd/^{144}Nd$ ratios based on their age and Sm/Nd composition (eg, DePaolo & Wasserburg, 1976). Oceanic crustal rocks recently derived from the mantle are characterized by relatively high Sm/Nd values, and hence radiogenic or relatively high $^{143}Nd/^{144}Nd$ values. Conversely, older and more felsic continental crustal rocks are characterized by lower ratios of the parent to daughter resulting in unradiogenic or low $^{143}Nd/^{144}Nd$ and ε_{Nd} values.

The dominant source of dissolved Nd to the oceans comes from the weathering and drainage of subaerially exposed rocks (Piepgras et al., 1979). Variations in seawater Nd are a result of the type of rock weathered and drained into a given ocean basin (Goldstein and Jacobsen, 1987). The initial ε_{Nd} signature of a particular water mass changes as it comes into contact with other waters masses (Piepgras and Wasserburg, 1982, 1987, Piepgras and Jacobsen, 1988, Jeandel et al., 1995, 1998, Amakawa et al., 2000), however due to the short residence time of Nd (~1000 years [Tachikawa et al., 1999]) relative to oceanic mixing (~1500 years [Broecker et al., 1960]), provenance Nd information is retained. Thus distinct interbasinal differences in Nd isotope composition develop between different oceanic water masses and basins.

Modern North Atlantic Deep Water (NADW) has an ε_{Nd} value of -14 (Piepgras and Wasserburg, 1987), which reflects the weathering input of ancient Canadian Shield rocks into the Labrador Sea. Pacific deep waters are characterized by ε_{Nd} values of ~ -4 to -5 (Piepgras and Jacobsen, 1988) imparted by weathering and drainage of young, circum-Pacific volcanic terranes. Southern Ocean water masses, Antarctic Bottom Water (AABW) and Antarctic Intermediate Water (AAIW), have intermediate ε_{Nd} values ~ -8 (Piepgras and Wasserburg, 1982; Jeandel, 1993) due to the mixing between Pacific and

Atlantic seawater. It is important to note that while modern Pacific deep waters have a characteristic Nd isotope signal, deep-water formation does not occur in the North Pacific in the current mode of MOC. The "Pacific" deep-water signal of ~-4 to -5 is the result of vertical exchange between Pacific Intermediate water and the northward advecting circumpolar deep water.

In order to exploit Nd as a water mass tracer to reconstruct ancient deep-water circulation patterns, we need a phase that commonly accumulates in sediments and that records and retains the ancient seawater Nd isotopic composition. Several investigations of paleo-Nd isotopic composition used analyses of Fe-Mn crust layers (e.g., Ling et al., 1997, O'Nions et al., 1998, van de Flierdt et al., 2004), which precipitate directly from seawater. Although these crustal records laid the initial framework for reconstructing ancient water masses, Fe-Mn crust precipitate very slowly (~few mm per m.y.) and only provide limited geographic coverage of ocean basins. As an alternative, fossil fish teeth and bone (debris) are useful for paleo-Nd investigations because they occur in nearly all types of sediments (e.g., Arrhenius et al., 1957), are characterized by high concentrations of REEs (Wright et al., 1984; Shaw and Wasserburg, 1985; Staudigel et al., 1985), and they are resistant to dissolution in corrosive bottom waters (Person et al., 1995; Martin and Scher, 2004). Fish debris acquires elevated Nd concentrations during an early digenetic reaction at the water/sediment interface (Staudigel et al., 1985, Reynard et al., 1999). The Nd isotopic composition recorded in the fossil fish material thus derives from the water mass bathing the seafloor at a given location (Wright et al., 1984; Shaw and Wasserburg, 1985; Staudigel et al., 1985; Martin and Haley, 2000).

2.4 *Current State of Pacific Paleoceanographic Reconstructions*

Existing fossil fish debris and Fe-Mn crust Nd isotope data from the tropical Pacific spanning the interval ~70 to ~35 Ma indicate intermediate- and deep-water mass compositions with relatively radiogenic values, typically ranging between -3 to -6 epsilon units (Thomas, 2004; Thomas et al., 2008; van de Flierdt et al., 2004; Ling et al.,

1997, 2005). Records from currently located in the subtropical North Pacific, indicate overall ε_{Nd} trends and values similar to each other, suggesting that both sites shared a common deep-water mass. The long term trends recorded at Ocean Drilling Program (ODP) Sites 1209 and 1211, paleodepth ~2,300 m and ~2,900 m respectively, suggest that deep waters in the central tropical Pacific evolved from relatively radiogenic compositions (ε_{Nd} ~4.5), to more radiogenic values (ε_{Nd} ~3-3.5) from ~65- 45 Ma and then back to lower "background" values beginning ~45Ma. Thomas (2004) proposed that the deep tropical Pacific was a mixing location of water masses that convected in both the Southern Ocean and North Pacific, with convection in the North Pacific beginning/intensifying over the interval ~65 to 45 Ma based on the increase in Nd isotope values. Weathering and drainage of Northern Pacific island arc terranes likely was the source of the radiogenic dissolved Nd to the late Cretaceous and early Paleogene oceans, as arc volcanism had been underway since at least ~110 Ma (Larson and Pitman, 1972). The ~20 million year interval characterized by higher deep-water Nd compositions suggests a more efficient transfer of radiogenic Nd from surface waters to the deep North Pacific. The simplest explanation for more efficient transfer of radiogenic Nd to deep waters is convection in the Northern Pacific during the early Paleogene (Thomas, 2004).

More recent Nd isotope values recorded in both fish debris and detrital silicate sediments from six North Pacific DSDP and ODP sites, combined with coupled model simulations confirms a North Pacific source for the radiogenic Nd to the Pacific (Hague et al., in review). Northern Pacific intermediate- and deep-water Nd isotope values ranged from ~-5.6 to +3.7, suggesting that seawater values generally were higher in the North Pacific than compared to the tropical Pacific. Fully coupled model simulations predict convection in both the South and North Pacific for a relatively "cool" Paleocene run as well as a "warm" Eocene simulation, with potential intensification of convection in both regions of the Pacific from ~67-55 Ma (the "cool" simulation) (Hague et. al., in review).

Limited data supports deep-water formation in the Atlantic sector of the Southern Ocean during the early Paleogene. Seismic records linked an erosional event in the western North Atlantic to southern ocean influenced bottom-water formations in the Paleocene Period (Mountain and Miller, 1992). In addition, benthic foraminiferal faunal turnover suggests convection in the Southern Ocean during the early Paleogene (Pak and Miller, 1992). Nd isotope values of the early Paleogene Southern Ocean also support the dominance of a Southern Ocean deep-water source in the Atlantic basins based on the trends and values of existing data, combined with tectonic and hydrographic constraints (Thomas et al., 2003). However the Nd isotopic composition of the inferred Atlantic sector Southern Ocean source is much lower than values recorded in the Pacific (~-9), suggesting that this water mass did not impact the deep tropical or North Pacific.

Existing data from the tropical Pacific also suggest that deep waters from the Atlantic did not circulate through the Caribbean gateway into the Pacific basin deep waters (Thomas et al., 2008). However the current data set cannot rule out any intermediate- or deep-water contribution of relatively warm and saline waters from the Tethys. Furthermore, the body of data is not able to constrain potential regions of deep-water formation in Southern Ocean during the early Paleogene. This is because the current geochemical data set lacks any sites or crusts from the high southern latitudes. Thus in order to indentify a Southern Ocean source in the Pacific we need to investigate high latitude locations from the Southern Pacific. To this end, we have generated new fossil fish debris Nd isotope records from the southern portion of the Pacific Ocean from Ocean Drilling Program (ODP) and Deep Sea Drilling Project (DSDP) Sites 323 and 596, as well as additional tropical Pacific Sites 463, 865, and 869. This study extends the paleogeographic coverage of the Late Cretaceous-Early Paleogene interval to ~65°S, spanning paleo water depths of 1500m to 5000m (Figure 1).

3. SITE SELECTION AND METHODS

3.1 *Site Selection and Stratigraphic Recovery*

DSDP Site 323 is situated in the central part of Bellingshausen abyssal plain in the eastern portion of the Pacific sector of the Southern Ocean (63°40.84'S, 97°59.69'W) at a water depth of 4993 meters. The paleo-latitude for Site 323 at ~ 63 Ma was 67°S (figure 1), and the paleodepth evolved from ~2000m during the Late Cretaceous and Early Paleocene to nearly 4000 meters (~35 Ma) (Rogl, 1976). The stratigraphic section spanning the study interval was recovered in cores 14 through 15 (638.00- 660.41 mbsf). Much of the sediments cored were deposited below the carbonate compensation depth (CCD), consequently most of the Eocene- Maastrichtian section lacks carbonate microfossils (Rogl, 1976). Accumulation rates for this sedimentary section were also very low, < 1 cm/1000 yr (Rogl, 1976). There is also a hiatus spanning most of the Eocene in cores 14 through 15 starting at ~637.67 to ~661.09 mbsf (Rogl, 1976), through most of the stratigraphic section containing the study interval.

DSDP Site 463 is located on the northwest Mid-Pacific Mountains (21°21.01'N; 174°40.07'E) in 2525 meters of water. Its paleodepth was ~2000 meters (~50 Ma) and paleolatitude was ~10˚N (Figure 1). The upper Maastrichtian to upper Eocene stratigraphic interval (41.41-47.84 mbsf) consists of foraminiferal and nannofossil chalk recovered in cores 6 through 7. A ~17 m.y. hiatus exists between the Oligocene and middle Eocene sections (Thiede et al., 1978). In the extremely condensed section of core 6 and the upper 3.3m of core 7 (~41.00 to ~43.00 mbsf), there is a hiatus between the middle Eocene and the Oligocene. There is also a short hiatus in core 7, section 3 (~46.80 mbsf), which encompasses most of the lower Eocene, and the entire Paleogene stratigraphic sections of the study interval (Thiede et al., 1978).

DSDP Site 596 is located in the southwest Pacific Ocean (23°51.20'S, 165°39.27'W) at a water depth of 5614 meters. This site paleodepth was ~5000 meters at 38°S (Figure 1) in the South Pacific during the Paleocene (~54-62 Ma). The upper Cretaceous to upper

Eocene stratigraphic section was only recovered in core 3 (16.74-23.83 mbsf) (the) and consists of brown, zeolitic clay lacking biostratigraphically useful microfossils (Winfrey et al., 1987).

ODP Hole 865B was drilled on Allison Guyot (18°26.41 'N, 179°33.34'W), in the Mid-Pacific Mountains at a water depth of 1530 meters. This site was located at or near the equator, ~5°N (Figure 1) throughout the Paleocene and Eocene (~62- 36 Ma) and at a paleodepth of 1500 meters (Sager et al., 1993). The study interval spans the upper Paleocene to upper Eocene, between 18.15-134.32 mbsf and was recovered in cores 3 though 15. The Paleogene sedimentary section consists of foraminiferal nannofossil ooze (Sager et al., 1993), with nearly complete recovery of the Paleogene (Bralower et al., 1995).

ODP Hole 869A was cored at Wodejebato Guyot in the equatorial Pacific Ocean (ll°0.091'N, 164°44.969'E) at a water depth of 4826.7 meters. Site 869 was situated at the equator (Figure 1) at a paleodepth of 3600m during the Eocene (~45 Ma) (Sager et al., 1993). The sampling interval for this investigation spans the upper Eocene to middle Eocene from 87.65-139.41 mbsf recovered from cores 10 through 15. The lithology is predominantly a clayey nannofossil and radiolarian ooze. Calcareous nannofossil biostratigraphy of Hole 869A indicates a hiatus in the upper middle Eocene and possibly also in the lower Oligocene (Firth, 1995).

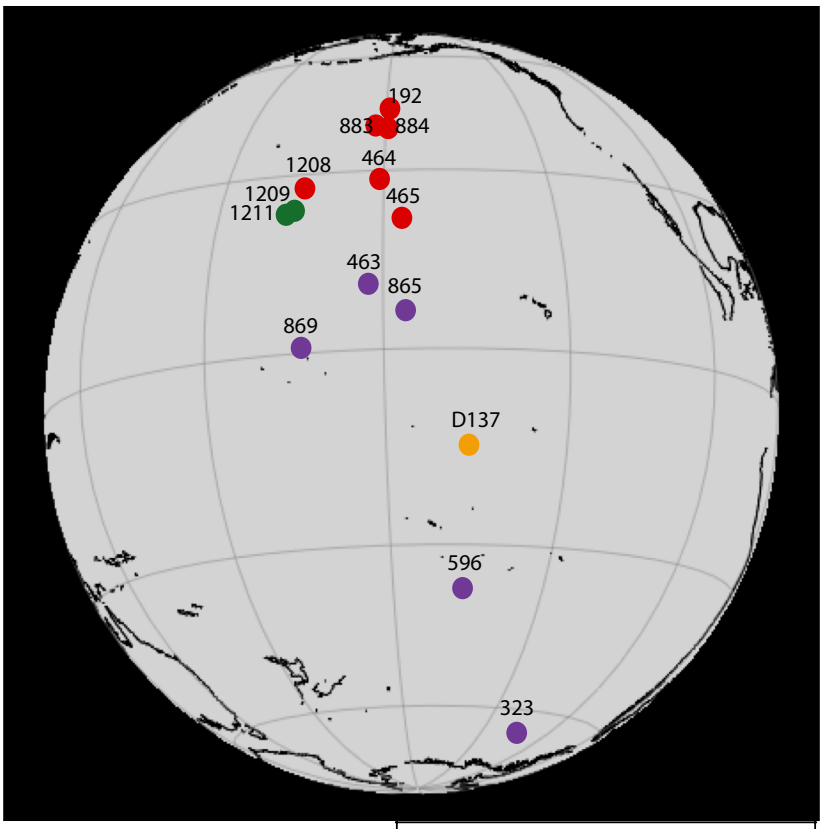

323	~4000m	192	~2500m
463	~2000m	464	~4000m
596	~5000m	465	~900m
865	~1500m	883	~2000m
869	~3600m	884	~3300m
D137	~7129m	1208	~3300m
1209	~2300m	1211	~2900m

Figure 1. Paleogeographic reconstruction 50Ma. Location of DSDP and ODP site locations; published data-red (Hague et al., in review), orange (van de Flierdt et al., 2004) and green circles (Thomas, 2004), purple circles-this study.

3.2 *Age Model*

Site 323

Biostratigraphically useful microfossils are rare throughout this section. Thus we had to use the closest biostratigraphic datums bounding the clay interval (our study section) highest datum below the clay interval and the lowest datum above the clay interval as the best available age control tie points. Shipboard nannofossil biostratigraphy identified species characteristic of NP2 and NP3 in sample 15-6, 16-18 cm (662.66 mbsf). Without any other constraints we estimated that sample to be of middle NP3 age, and thus we assigned an age of 63 Ma to 662.66. The shipboard biostratigraphers assigned the Core 7 core catcher sample (632.77 mbsf) an age of 15 Ma based on the identification of the diatom *Denticula nicobarica* [Hollister et al., 1976], and we apply this as the youngest age model tie point. Because no other age control exists for this red clay section, we linearly interpolated between these two tie points and assumed a constant sedimentation rate between the two datums.

Site 463

Although sediments recovered at Site 463 contain abundant carbonate microfossils, no detailed biostratigraphy exists. Shipboard lithologic description and biostratigraphy identified a hiatus in Core 7 section 3 spanning the middle Eocene to Maastrichtian [Thiede et al., 1978]. We used the shipboard nannofossil report for Paleogene ages above the unconformity [Thiede et al., 1978]. The report only provides an estimate of the nannofossil zone of the recovered sections, therefore we had to estimate the top and base of the respective zones, deriving the numeric ages from Berggren et al. [1995]. Below the unconformity we used Sr isotope ages from Barrera and Savin [1999]. See Table 1. for datum information.

Table 1. Datums for Site 463 age model.

Site 463					
Core	**Depth (mbsf)**	**Source**	**NP Zone and Biomarker**	**Age**	**Source**
Top 6	38.00	[Thiede et al., 1978]	Top NP 23	29.7	*Berggren et al [1995]*
Base 6	43.20	[Thiede et al., 1978]	Base NP 23	31.50	*Berggren et al [1995]*
6 cc		[Thiede et al., 1978]	NP 16	(40.2-43.3)	*Berggren et al [1995]*
7-1	43.5	[Thiede et al., 1978]	Top NP 13	49.60	*Berggren et al [1995]*
7-3	46.8	[Thiede et al., 1978]	Base NP 13	50.60	*Berggren et al [1995]*
7-3	46.94	[Barrera and Savin 1999]	*Sr isotope*	67.88	*Berggren et al [1995]*
7-3	47.84	[Barrera and Savin 1999]	*Sr isotope*	67.91	*Berggren et al [1995]*

Site 596

The brown clay lithology lacks biostratigraphically useful microfossils and ichthyolith assemblages yield uncertain and coarse temporal resolution (Winfrey et al., 1987). Thus we used the Zhou and Kyte (1992) constant Co accumulation age model for Site 596.

Site 865B

A detailed Paleogene nannofossil biostratigraphy exists for Hole 865B (Bralower et al., 1995) and we used the numeric ages from the Berggren et al. (1995) timescale. See Table 2. for datum information.

Table 2. Datums for Site 865B age model.

Site 865B		
Biomarker Datums	**Depth**	**Age (Ma)**
	(mbsf)	
LO *Discoaster barbadiensis*	18.70	34.30
LO C *Chiasmolithus grandis*	19.32	37.10
LO *Chiasmolithus solitus*	29.40	40.40
FO R. *umbilicus*	47.31	43.70
FO C *Chiasmolithus gigas*	67.70	44.50
FO *Discoaster sublodoensis*	79.60	49.70
LO *Tribrachiatus orthostylus*	79.60	50.60
FO *Discoaster lodoensis*	89.60	52.85
LO M. *velascoensis*	100.90	54.70
FO *Discoaster multiradiatus*	116.21	56.20
FO *Discoaster mohleri*	125.75	57.50
FO F. *tympaniformis*	132.20	59.70

Site 869A

We used the nannofossil datums identified by Firth (1995) with ages from Berggren et al. (1995) to create the Site 869 age model (Table 3).

Table 3. Datums for Site 869A age model.

Site 869A		
Biomarker Datum	**Depth**	**Age (Ma)**
	(mbsf)	
LO *Chiasmolithus. grandis*	88.16	37.1
LO *Chiasmolithus solitus*	96.00	40.4
FO R. *umbilica*	*109.02*	43.7
FO *Chiasmolithus gigas*	141.93	46.1

3.3 *Analytical Methods*

Bulk sediment samples were disaggregated in a dilute solution of sodium metaphospate solution and washed through a >63 micron (μm) sieve. Teeth and fragments of fish debris were hand picked and ~20-30 fragments per sample depending on availability and size were used for each sample analysis. Replicate samples were also picked from several sites to confirm reproducibility. A select few samples underwent an oxidative/reductive cleaning stage process described in Boyle (1981). The oxidative/reductive cleaning protocol has been used to remove any oxide coating and residual organic matter from the fish debris prior to dissolution (Boyle, 1981; Boyle and Keigwin, 1985), however recent work indicates that the oxides coating records the Nd isotopic composition of the water mass bathing the seafloor at a given location (Martin et al., 2010; Roberts et al., 2010; Hague et al., in review), which is the same signal recorded by biogenic apatite. To validate this finding for our South Pacific samples we also compared a subset of samples cleaned with the Boyle oxidative/reductive method (C) with a separate split that was rinsed twice in ethanol followed by two rinses in ultrapure water (Milli-Q) (UC). Results from two analyzed samples at each site using each method verified that the Boyle cleaning was unnecessary, and we eliminated the reductive/oxidative cleaning step for the remainder of the samples.

Fish debris samples were dissolved in 2N HNO_3 and rare earth elements (REE) were isolated using RE Spec cation exchange column chemistry followed by Nd isolation from the bulk rare earth elements via methyllactic acid column chemistry. The entire analytical procedure is described in Appendix A.

We also analyzed the Nd isotopic composition of the seawater-derived Fe–Mn oxyhydroxide fraction. Bulk sediment was dried, homogenized and then decarbonated using buffered dilute acetic acid. Next, buffered and chelated 0.02 M hydroxylamine hydrochloride (HH) solution was added to each sample and placed on the shaker table 1.5 hours. The leachate (dissolved oxide fraction) was dried down and then processed

through the two-stage column chemistry described above. To the remaining solid residue we added additional HH solution again and placed on the shaker for 24 hours. The samples were rinsed three times before being dried down and repowdered. Approximately 50 mg of detrital powder was thoroughly digested in concentrated HNO_3 and HF, and then HCl. Dissolved samples were processed through two-stage column chemistry.

All samples were loaded using 1ul of 2N HCL onto a rhenium (Re) filament and analyzed on the Thermo Triton thermal ionization mass spectrometer as Nd^+. External precision was 12ppm (2σ) with a value 0.512104 based upon replicate analysis of JNd_i standard (n=50) over the course of this study. $\varepsilon_{Nd}(t)$ values were calculated using the numerical ages determined with the age models detailed above. For fish debris, we applied a typical $^{147}Sm/^{144}Nd$ value of 0.131 after Thomas et al. (2008). We adopted the $^{147}Sm/^{144}Nd$ value of 0.109 for determination of the silicate $\varepsilon_{Nd}(t)$ values based on upper crustal average concentrations of Sm and Nd (Taylor and McClennan, 1995), and a $^{147}Sm/^{144}Nd$ value of 0.115 for the oxide fraction based on values reported for Fe-Mn crusts (e.g., Ling et al., 1997).

4. RESULTS

4.1 *Site 323*

The $\varepsilon_{Nd}(t)$ values recorded by the uncleaned samples range from -5.0 to -6.4 throughout the study interval (Figure 2; Appendix B). Values gradually increase from -5.6 at 660.41 mbsf (59.5 Ma) to -5.0 at 657.84 mbsf (55.4 Ma) and then decrease to-6.4 at 638 mbsf (23.4 Ma). Comparison of Nd isotopic values of cleaned samples with the respective uncleaned values indicates similar values (Appendix B): the cleaned fraction from sample 14-4, 141-143 had an $\varepsilon_{Nd}(t)$ value of -5.9 while the uncleaned fraction was also -5.9. The cleaned fraction from sample 15-1, 121-123 had an $\varepsilon_{Nd}(t)$ value of -5.3 while the uncleaned fraction was -5.3, and cleaned fraction from sample 15-3, 39-41 had an $\varepsilon_{Nd}(t)$ of -5.0, while the uncleaned was -5.4 (the 0.4 epsilon unit difference is similar to the external reproducibility). Two analyses of the oxide fraction leached from bulk sediment recorded an $\varepsilon_{Nd}(t)$ value of -5.9 at 638.91 mbsf and -4.9 at 660.41 mbsf. Four silicate analyses from Site 323 yielded $\varepsilon_{Nd}(t)$ values of -3.6 at 638.91 mbsf (24.9 Ma) to -3.6 at 657.39 mbsf (54.7 Ma) to -3.9 at 659.40 mbsf (57.9 Ma) and -4.0 at 660.41 mbsf (59.5 Ma), and record a general increase up section.

4.2 *Site 463*

The $\varepsilon_{Nd}(t)$ values recorded by the uncleaned sample range from -3.7 to -6.4 throughout the study interval (Figure 2, Appendix B). Values decreased from -4.9 to -5.1 between 47.84 and 47.65 mbsf (~67.9 Ma), then increased to ~3.8 between 46.61 and 43.98 mbsf (50.54 -31.10 Ma). From 46.02 to 43.98 values remained relatively constant between -3.7 and -3.9, but decreased to -6.4 at 42.58 mbsf (30.7 Ma), and increased to -4.1 by 41.41 mbsf (30.5 Ma). Comparison of Nd isotope value of one cleaned sample with the respective uncleaned values indicate similar values (Appendex B): the cleaned fraction from sample 7-3, 115-117 had an $\varepsilon_{Nd}(t)$ value of -5.0 while the uncleaned fraction was -5.1. Five analyses of the oxide fraction leached from the bulk sediment recorded an $\varepsilon_{Nd}(t)$ value of -4.9 at 46.94 mbsf (67.8 Ma), -3.8 at 45.55 mbsf, -3.9 at 43.98 mbsf (31.1 Ma),

-3.8 at 42.58 mbsf (30.7Ma), and -4.0 at 41.41mbsf (30.5 Ma).One silicate analysis from Site 463 yielded $\varepsilon_{Nd}(t)$ value of -12.2 at 46.94 mbsf (67.88Ma).

4.3 *Site 596*

The $\varepsilon_{Nd}(t)$ values recorded by the uncleaned sample generally range from -6.0 to -5.1 throughout the study interval with little stratigraphic trend (Figure 2; Appendix B). However one sample recorded a transient increase to -3.6 at 17.92 mbsf (57.0 Ma). Comparison of Nd isotope value of the cleaned samples with the respective uncleaned values indicates similar values (Appendix B): the cleaned fraction from sample 3-2, 141-143 had an $\varepsilon_{Nd}(t)$ value of -5.8 while the uncleaned fraction was -5.6. Two analyses of the oxide fraction leached from the bulk sediment recorded an $\varepsilon_{Nd}(t)$ value of -5.4 at 20.37 mbsf (67.49 Ma) and -5.2 at 16.74 mbsf (50.89 Ma). Four silicate analyses from Site 596 yielded $\varepsilon_{Nd}(t)$ values of -8.1 at 20.37 mbsf (67.49 Ma), to -9.0 at 19.24 mbsf (63.06 Ma), to -8.5 at 18.41 mbsf (59.46 Ma) and -6.9 at 16.74 mbsf (50.98 Ma).

4.4 *Site 865B*

The $\varepsilon_{Nd}(t)$ values recorded by the uncleaned samples ranged from -3.1 to -4.8 throughout the study interval (Figure 2; Appendix B). Between 134.32 and 73.81 mbsf (60.43 - 47.95 Ma), $\varepsilon_{Nd}(t)$ values averaged ~-4.4, and then increased to - 3.1 by at 50.57 mbsf (44.08 Ma). Subsequently, $\varepsilon_{Nd}(t)$ values decreased to -4.3 at 21.56 mbsf (37.82 Ma) and remained between -4.4 and -4.5 to the top of the study interval (18.15 mbsf). Three analyses of oxide fraction leached from bulk sediment recorded an $\varepsilon_{Nd}(t)$ value of -3.9 at 116.63 mbsf (56.20 Ma), -4.2 at 108.98 mbsf (55.49 Ma) and -4.4 at 19.40 mbsf (37.12 Ma).

4.5 *Site 869A*

The $\varepsilon_{Nd}(t)$ values recorded by the uncleaned sample ranged from -4.2 to -4.6 throughout the study interval (Figure 2; Appendix B) and exhibit no significant stratigraphic trend. Comparison of the Nd isotopic values of cleaned samples with the respective uncleaned

values indicates similar values (Appendix B): the cleaned fraction from sample 10-2, 91-93 had an $\varepsilon_{Nd}(t)$ value of -4.5 while the uncleaned fraction was also -4.5. Two analyses of the oxide fraction leached from the bulk sediment recorded an $\varepsilon_{Nd}(t)$ value of -5.1 at 138.59 mbsf (45.88 Ma), and -4.6 at 87.65 mbsf (37.07 Ma). One silicate analyses from Site 869A yielded $\varepsilon_{Nd}(t)$ values of -6.0 at 87.65 mbsf (37.07 Ma).

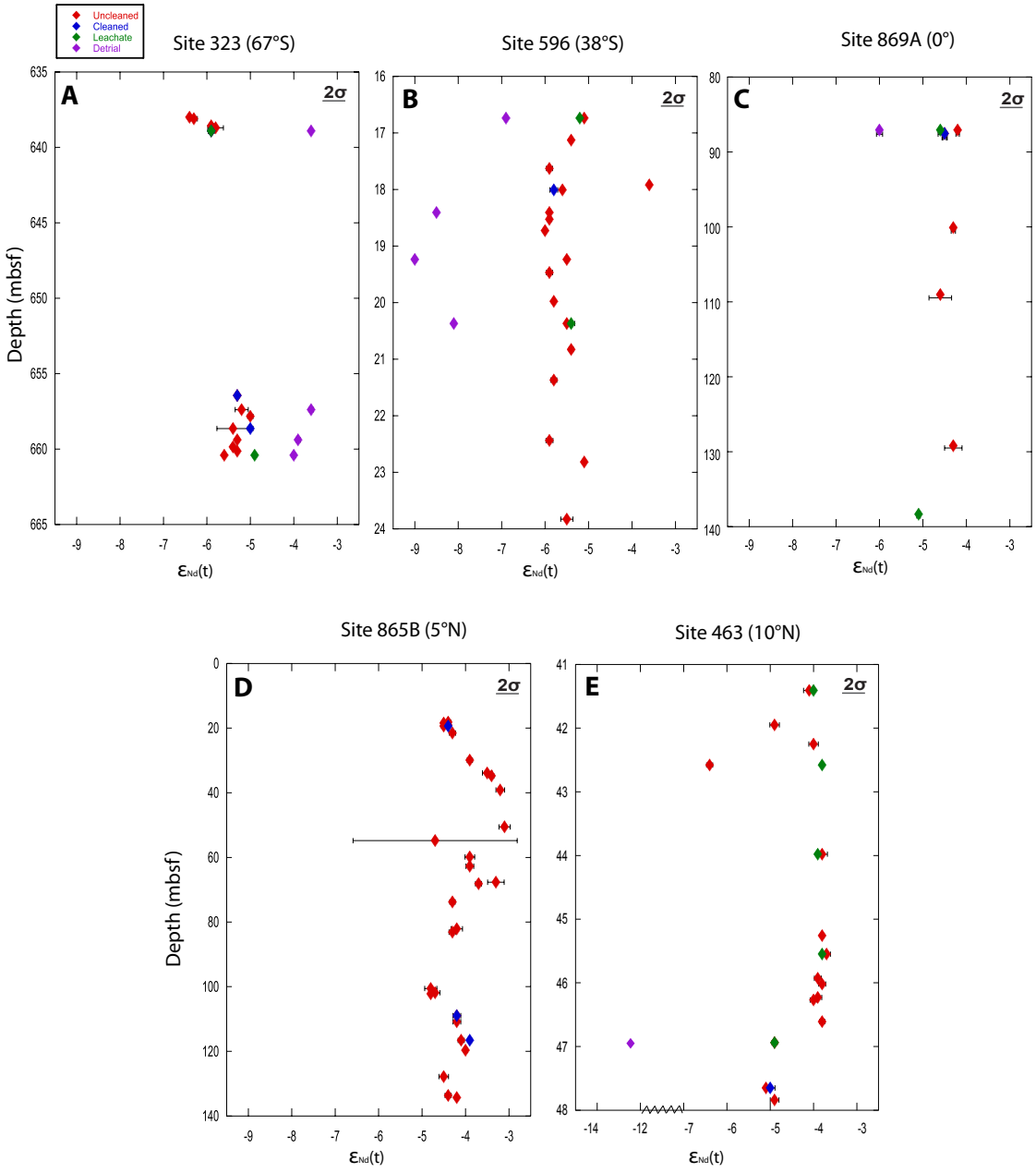

Figure 2. South Pacific Data generated in this study.

5. DISCUSSION

5.1 *South Pacific Detrital Silicate Sources*

Detrital sediments that accumulate on the seafloor in pelagic environments are delivered by wind, rivers and hemipelagic processes. The Nd isotopic composition of the detrital sediments reflects the composition of the rocks from which those sediments weathered, and thus may help constrain the source(s) of the detrital material. Detrital silicate $\varepsilon_{Nd}(t)$ values recorded at the five study sites throughout the ~50 Myr study interval range from -3.6 to -12.2, with a median value of -6.5 (Figure 3). This range of values suggests at least one radiogenic source and at least one unradiogenic source of detrital sediments, and intermediate values likely reflect mixing of radiogenic and unradiogenic components. Of the five study sites, only Site 323 was located sufficiently close to land to have been impacted by fluvial or hemipelagic inputs of detrital sediments (Figure 1). The other sites were all located far from land toward the center of the tropical Pacific basin, thus the only likely source of detrital materials to those sites was eolian, either continentally-derived dust and/or volcanic ash.

Site 323 recorded the most radiogenic detrital silicate $\varepsilon_{Nd}(t)$ values (-3.6 to -4.0) (Figure 3). These values likely reflect proximity to the Antarctic Peninsula. The Antarctic Peninsula was the site of long-term subduction of the proto-Pacific plates during the Mesozoic and Cenozoic (e.g., Barker, 1982). While the nature and composition of the subduction-related volcanics were diverse (e.g., Pankhurst, 1990; Storey et al., 1992), The Nd isotopic composition of various exposed rocks along the Antarctic Peninsula is radiogenic with $\varepsilon_{Nd}(t)$ values ranging from ~-6 to ~+5 (e.g., Wareham et al., 1997; Riley et al., 2001). Weathering of these terranes likely supplied radiogenic detrital sediments to Site 323 region.

The detrital Nd isotopic composition recorded at Site 596 ranged from -9.0 to -6.9 epsilon units (Figure 3). This range of values is consistent with a relatively unradiogenic source of dust with a potential contribution of more radiogenic volcanic ash in the uppermost sample analyzed (Figure 2, Panel B). The paleo-latitude of Site 596 was ~38°S during the study interval, placing the region within the general influence of the Southern Hemisphere westerlies. A likely source of dust would have been Australia, however much of Australia was humid during the early Paleogene (Martin, 2006), and Australian dust likely would have had relatively low Nd isotopic values. But the inferred humid conditions in Australia could account in part for the low rate of sediment accumulation in the southern Pacific during the Late Cretaceous and much of the Paleogene (e.g., Zhou and Kyle, 1992; Rea et al., 2006).

Equatorial Pacific Site 869 recorded a detrital silicate $\varepsilon_{Nd}(t)$ value of -6 at 37.07 Ma (Figure 3). This value suggests a possible mixing of unradiogenic dust and more radiogenic ash, or from dust/ash derived from andesitic type arc terranes. Situated at a tropical paleo-latitude, Site 869 was likely influenced by either the northeast or southeast trades. Therefore both the radiogenic and unradiogenic contributions derived from the east. The Caribbean, Central American, and South American regions experienced active plateau and arc volcanism throughout much of the Cretaceous and early Cenozoic (e.g., Kerr et al., 2002). Ashes from these regions could have supplied both radiogenic dust and andesitic, less radiogenic ash/dust to the central Pacific, while semi-arid and arid regions of Northern Africa could have supplied the unradiogenic dust to the tropical Pacific (Zaier et al., 1998).

One detrital sample analyzed from Site 463 yielded a $\varepsilon_{Nd}(t)$ value of -12.2 at 67.9 Ma (Figure 3), and this is the most unradiogenic detrital value in the data set. This value is consistent with delivery of unradiogenic eolian dust to the region and is lower than the Nd isotopic composition of eolian dust analyzed at nearby sites. Woodard and Thomas (in prep) analyzed the composition of dust from ODP Site 1209 and found values ranging from ~-10 to -11 over the interval ~58-59 Ma, and analyses from the giant piston core LL44-GPC3 in the Central North Pacific Ocean range from -10.2 to -6.5 over the interval 70 to 39 Ma (Pettke et al., 2002). Site 463 was located further south than either Site 1209 or the GPC3 and the source(s) of dust to the sites likely was influenced by the paleo-location of the Intertropical Convergence Zone (ITCZ) (e.g., Pettke et al, 2002). The unradiogenic dust deposited at Site 463 either derived from a Northern Hemisphere source to the east or a Southern Hemisphere source to the east. Dust derived from the Saharan region of Africa may be a possible source of unradiogenic εNd to the central Pacific region (Woodard and Thomas, in prep). Paleo-environmental reconstructions of Northern Africa indicate a semi-arid to arid climate during the Paleogene period (Jacobs et al., 1999; Zaier et al., 1998). These conditions could have produced dust that was transported by the trade winds across the central Atlantic Ocean to the tropical Pacific.

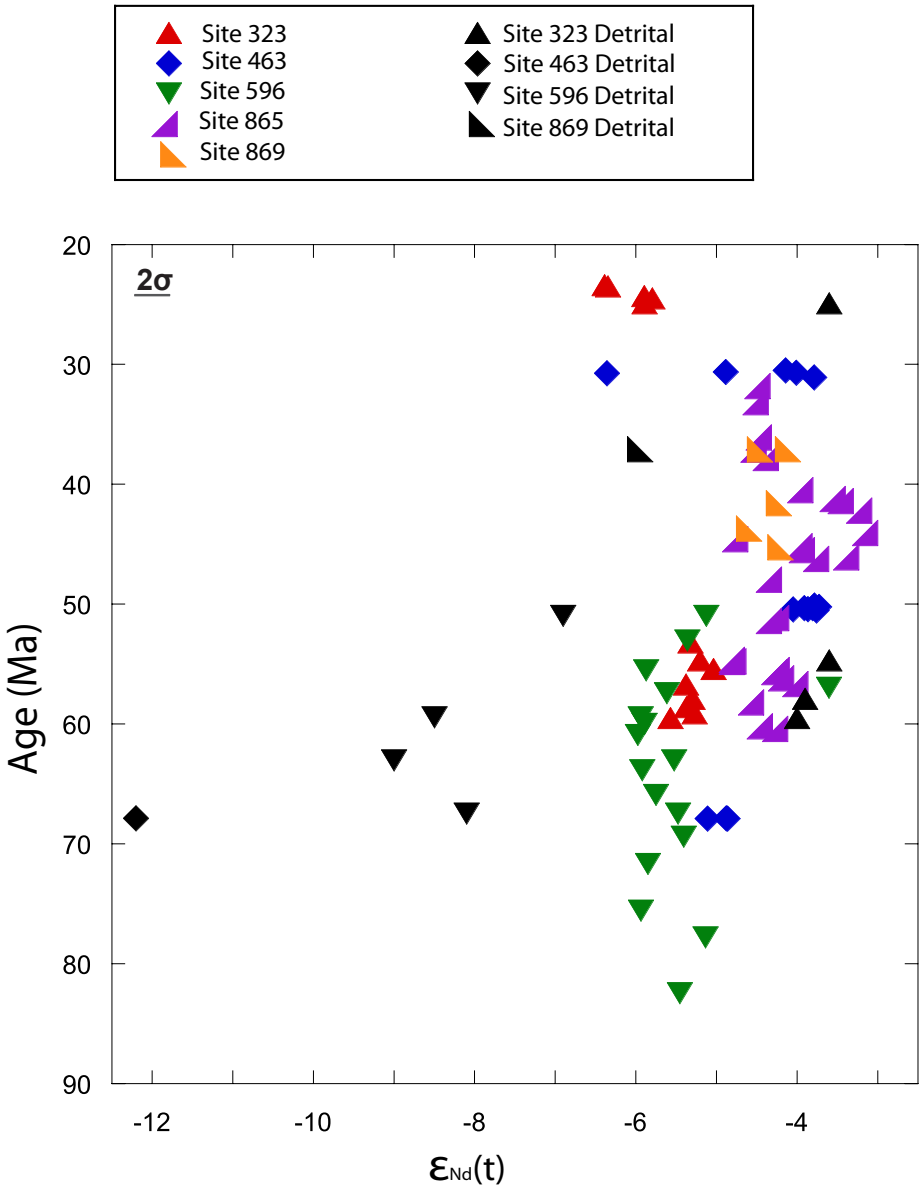

Figure 3. Nd isotope composition of extracted detrital silicates and fish debris.

5.2 *Evolution of South Pacific Water Mass Composition*

The average $\varepsilon_{Nd}(t)$ value recorded by fish debris at Site 323 is -5.6. Site 596 recorded the same average composition (-5.6). The average $\varepsilon_{Nd}(t)$ values recorded at Sites 869, 865 and 463 were -4.4, -4.1, and -4.3, respectively. Comparison of the mean isotopic values suggests a geographic trend in the water mass composition, with lower isotopic values in the temperate and high-latitude South Pacific and higher isotopic values in the tropical Pacific (Figures 3 and 4).

The similar Nd isotope values recorded at Sites 323 and 596 (where the two records overlap), as well as the southerly locations of the two sites, suggests that the same water mass bathed the two sites (Figures 3 and 4). From ~60-53 Ma, Site 323 $\varepsilon_{Nd}(t)$ values ranged from -5.6 to -5.0, and over the same general time interval, Site 596 $\varepsilon_{Nd}(t)$ values ranged from -5.9 to -5.4. The small isotopic offset between the two sites might reflect differences in location and/or water depth. The water depth at Site 323 during the Paleocene and Early Eocene was ~2000m while that at Site 596 was ~4000m. It is interesting to note that the water depth at Site 323 had increased to ~4000m by the Late Eocene, and the range of $\varepsilon_{Nd}(t)$ values recorded at Site 323 during the general interval ~25- 23Ma was -6.4 to -5.8. Alternatively, the same water mass could have bathed the entire depth range spanned by both sites during the Early Paleogene (~2000-4000m) and the subtle difference in isotopic composition recorded at the two sites was caused by small amounts of water mass mixing during the transit between the two regions. The overall higher values recorded at Sites 463, 865 and 869 potentially reflect the more northerly locations of those sites. For time intervals in which the records overlap, the three sites record similar values in spite of the large water depth range spanned (~1500 to 3600m).

Comparison of Nd isotopic values recorded in both fish debris and detrital silicate fractions at each of the study sites helps constrain the source(s) of dissolved Nd and hence, water mass composition(s), to the South and tropical Pacific (Figure 3). The Nd

isotopic composition of fine-grained detrital sediment transported by rivers is the same as that of the dissolved inventory (e.g., Goldstein et al. 1984; Goldstein and Jacobsen, 1988). The only study site that would have been impacted by fluvial inputs of detrital Nd was Site 323, thus Site 323 is the only site at which both the detrital and dissolved Nd could have been derived from regional weathering inputs. As discussed above, the radiogenic Nd isotopic composition of the detrital inputs at Site 323 likely reflects a significant weathering input from the Antarctic Peninsula (e.g., Riley et al., 2001). The isotopic composition of the fish debris (dissolved Nd) fraction was lower than the detrital values throughout the section at Site 323, and the average difference between the two fractions was ~1.8 epsilon units. However, the fact that the dissolved values are also relatively radiogenic likely reflects a contribution of dissolved radiogenic Nd from the Antarctic Peninsula. But the overall lower isotopic composition of the waters recorded at Site 323 indicates a contribution of more unradiogenic Nd as well, either from weathering of other Antarctic terranes (eg. van de Flierdt et al., 2004) or through advection of more unradiogenic waters into the study region. The consistent Nd isotope values recorded by both the fish debris and the detrital fractions at Site 323 suggests a consistent and relatively proximal source of dissolved and detrital Nd to the region.

Site 323 is the only site investigated that recorded higher detrital Nd isotopic values than dissolved Nd values. The observation that the more northerly sites recorded more radiogenic dissolved Nd isotopic values than the detrital fractions suggests that the source region(s) for these waters was (were) influenced by radiogenic Nd weathering inputs. Based on this study and previous work, the likely source regions for the water masses in the tropical Pacific were the high-latitude North Pacific (Thomas, 2004; Thomas et al., 2008; Hague et al., in review) and/or the high latitude South Pacific (this study). Furthermore, eolian inputs or boundary scavenging did not affect the Nd isotopic composition of the intermediate and deep waters at the study sites. Boundary scavenging is common in depositional environments characterized by high productivity (Lacan and Jeandel, 2005; Murphy and Thomas, 2010). Only Site 869 recorded

relatively high abundances of siliceous microfossils indicative of high equatorial productivity (Berger et al., 1981; Sager et al., 1993), but the fact that the dissolved Nd isotopic composition was similar to the values recorded at Sites 463 and 865 suggests that scavenging of surface water Nd to the seafloor at Site 869 was not significant.

The key features in the data -the northerly increase in dissolved Nd isotopic composition (Figure 4), the coherence and consistency of the Site 323 dissolved and detrital Nd isotope values, the decoupling of tropical Pacific dissolved and detrital values- are best explained by convection of deep waters in the Pacific sector of the Southern Ocean that flowed northward. The more variable, but overall more radiogenic Nd isotope values of the intermediate and deep waters in the tropical Pacific (e.g., Thomas, 2004; Thomas et al., 2008; van de Flierdt et al., 2004; Ling et al., 1997, 2005; Hague et al., in review) reflected varying contributions both from the Southern Ocean as well as the North Pacific. The relatively radiogenic signature of this Southern Ocean source is likely unique to the Pacific sector, as previous work indicates that the Atlantic and Indian sectors were characterized by significantly lower isotopic compositions during the Late Cretaceous and Early Paleogene (e.g., Thomas et al., 2003; Scher and Martin, 2004; Murphy and Thomas, in revision). In order to distinguish the Pacific sector source from the rest of the Southern Ocean, we will refer to this water mass as "South Pacific Deep Water" (SPDW). The water signature associated with end-member SPDW was diluted during the transit northward to the tropical Pacific. Variations in the isotopic composition of tropical Pacific deep waters likely reflect variations in the contributions of SPDW versus more radiogenic deep waters from the North Pacific (North Pacific Deep Water – NPDW).

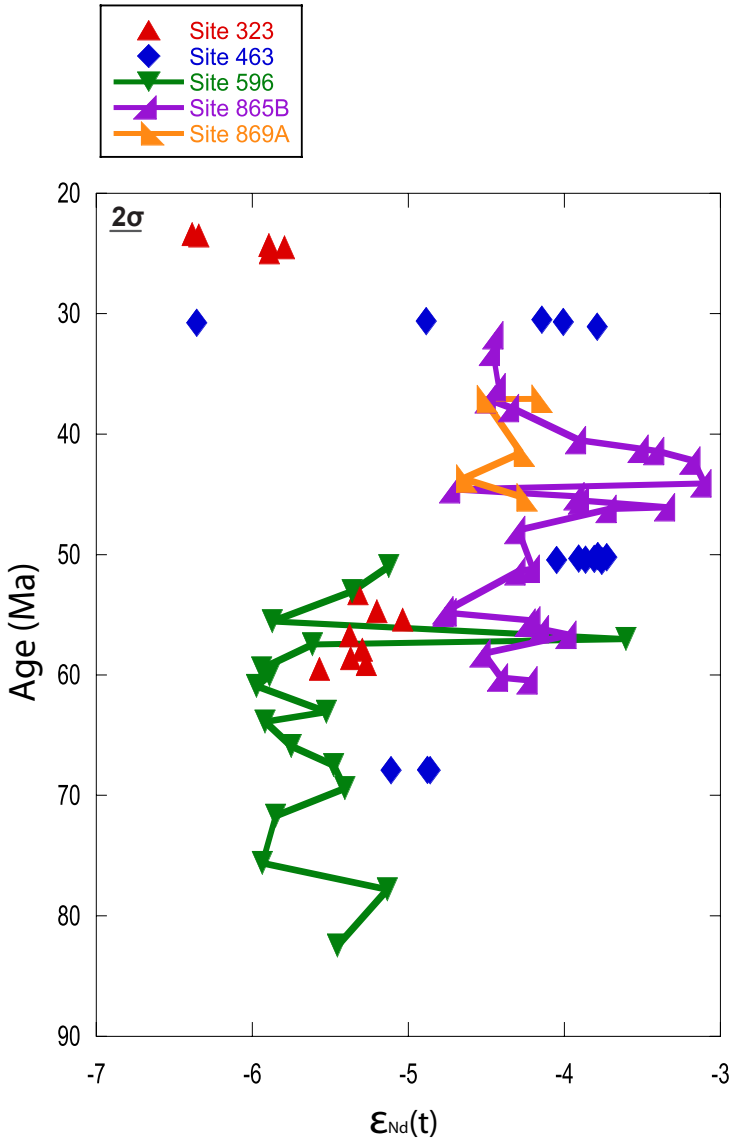

Figure 4. Dissolved Nd isotopic composition (this study). Derived from fish debris recorded at the five study sites plotted on a common age scale.

5.3 *Reconstruction of Pacific Ocean Overturning Circulation*

The new Nd isotope data presented here confirms the existence of the hypothesized Southern Ocean end-member postulated by Thomas (2004). The hypothesized southern source was based on the assumption that the tropical Pacific $\varepsilon_{Nd}(t)$ values reflect mixing of a radiogenic component from the North and an unradiogenic component from the South. Under modern conditions, Pacific deep waters are characterized by ε_{Nd} values of ~-4 to-5 (Piegras and Jacobsen, 1988), This composition results from the slow northward advection of Circumpolar Deep Water with ε_{Nd} values of ~-8 to -9 (Piepgras and Wasserburg, 1982; Jeandel, 1993), overprinted with scavenged radiogenic surface water Nd. Thus by the time Circumpolar Deep Water reaches the tropical Pacific its isotopic composition has increase by 4 to 5 epsilon units. We anticipated a Late Cretaceous – Early Paleogene southern source to have formed near the Ross Sea area with a relatively unradiogenic isotopic signature similar to the modern range of ~-8 to -9. However the $\varepsilon_{Nd}(t)$ values recorded from southern Pacific Sites 323 and 596 of ~-5 to ~-6 are significantly higher than hypothesized and must reflect a contribution of dissolved Nd from the Antarctic Peninsula region. This water mass may have convected in the Ross Sea region received relatively radiogenic dissolved inputs from the peninsula arc terranes.

The fact that the isotopic composition of SPDW is relatively radiogenic compared to modern Southern Ocean waters has significant implications for our understanding of oceanic heat transport during the Late Cretaceous and Early Paleogene. The gradual increase in $\varepsilon_{Nd}(t)$ values of just ~1 to 2 epsilon units from the SPDW source to the tropical Pacific implies relatively rapid advection of deep waters in the Pacific basin. In contrast, northward advection of a water mass with a "starting" composition of ~-8 to -9 epsilon units would imply more sluggish circulation to allow time for particle scavenging to overprint the isotopic composition by ~4 to 5 epsilon units. This new evidence for relatively vigorous Late Cretaceous and Early Paleogene overturning

circulation is consistent with recent early Paleocene dust data indicating more vigorous than expected wind intensities in the tropical Pacific (Woodard et al., 2011).

Comparison of the new records with the existing body of Paleogene Pacific data refines the current reconstruction of Pacific overturning circulation. The relatively constant dissolved values recorded throughout the study interval at South Pacific Sites 323 and 596 (with the exception of the single Site 596 value of ~-3.6 – additional data are required to assess this "excursion"), as well as the consistent detrital values recorded at Site 323, suggests that weathering inputs into the SPDW convection region were stable. It is difficult to assess potential changes in the flux of SPDW from Sites 323 and 596 alone. However, the overall distribution of Nd isotopic values within the tropical and subtropical North Pacific likely reflects the relative influence of convection in the northern (radiogenic) and/or southern (less radiogenic) source regions (Figure 5). Average $\varepsilon_{Nd}(t)$ values recorded at tropical Pacific sites and crusts proceeding from south to north are ~-5.2 at D137, ~-4.7 at VA13/2, -4.4 at Site 869, ~-4.3 at D11, ~-4.8 at CD29, ~-4.0 at CB12, ~-4.3 at CJ01, -4.1 at Site 865, ~-4.3 at Site 463, ~-4.2 at CLD01, -3.3 at Site 465, ~-3.7 at Site 1209, and ~-3.6 at Site 1211. Overall average values generally increased northward within the tropical Pacific supporting the geographic influence of more radiogenic waters from the north interacting with less radiogenic waters from the south.

Variations in the $\varepsilon_{Nd}(t)$ values recorded at the tropical sites/crusts may indicate changes in the relative contribution of waters from the North Pacific versus the South Pacific (Figure 5). For example, intervals of time characterized by an increase in the isotopic composition recorded by the tropical sites may reflect increased convection of North Pacific deep waters and/or diminished convection of SPDW. Sites 865 and Site 1209/1211 show relative isotopic increases over the interval ~60 to ~43 Ma. However, Site 865 $\varepsilon_{Nd}(t)$ values only overlap to ~-3 with 1209/1211 for a short period of time ~44 to 40Ma, indicating tropical Pacific Sites 1209 and 1211 $\varepsilon_{Nd}(t)$ values experience

"background" overlapping with the SPDW end-member water mass before and after Northern Pacific water mass influences. The temporal changes in $\varepsilon_{Nd}(t)$ values indicates the relative strength of the different water masses and their geographic extent. Northern Pacific waters likely did not influence past Site 865 since $\varepsilon_{Nd}(t)$ values did not go above -4. SPDW persisted in the South Pacific as more southern Sites 323, and 596 maintained constant seawater Nd values throughout the study interval. The overall $\varepsilon_{Nd}(t)$ trends in both northern and southern Pacific data supports bimodal convection of high latitude deep-water in the Pacific Ocean during the Late Cretaceous to Paleogene.

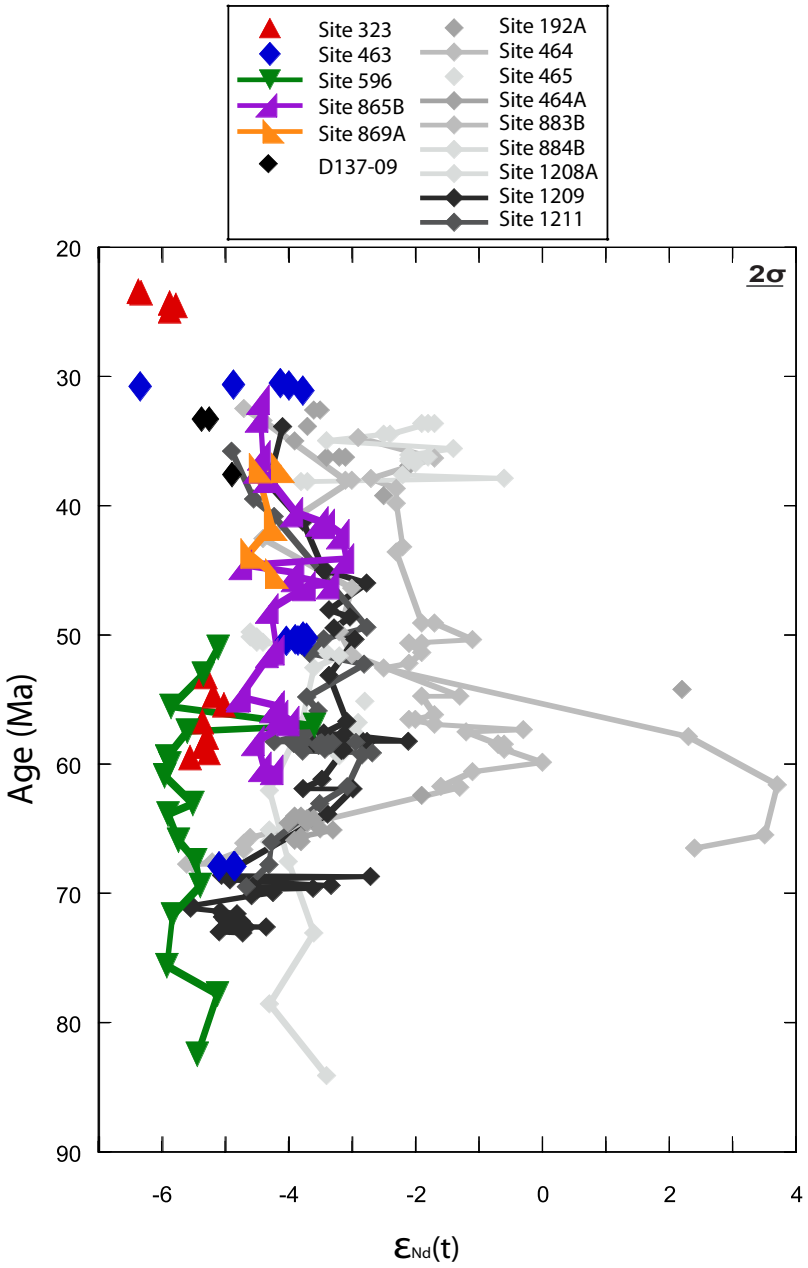

Figure 5. Previously published and new measure Nd isotope data. Previously published (grayed and black) shown with the new Nd isotope data from this study (colored)

6. CONCLUSIONS

1) Fossil fish debris and detrital silicate Nd isotope data from South Pacific DSDP Sites 323 and 596 suggest that deep waters convected in the Pacific sector of the Southern Ocean. We designate this water mass South Pacific Deep Water (SPDW).
2) The isotopic composition of SPDW was more radiogenic than hypothesized but is lower than the composition of waters sourced from the North Pacific.
3) New and existing tropical Pacific data indicate that the tropical Pacific was the location of water mass mixing between SPDW from the south and North Pacific Deep Water (NPDW) from the north.
4) Temporal variations in the dissolved Nd isotopic composition recorded at tropical and northern subtropical Pacific sites likely reflect variations in the contribution of NPDW relative to SPDW in the region.
5) The relatively radiogenic signature of SPDW and the small increase in the isotopic composition of deep waters during the transit north into the tropical Pacific implies a relatively rapid rate of deep-water advection.

REFERENCES

Amakawa, H., D. S. Alibo, and Y., Nozaki (2000), Nd isotopic composition and REE pattern in the surface waters of the eastern Indian Ocean and its adjacent seas, *Geochimica et Cosmochimica Acta, 64*, 1715-1727.

Arrhenius G., M.N. Bramlette and E. Picciotto (1957), Localization of radioactive and stable heavy nuclides in ocean sediments, *Nature*, *180*, 85-86.

Barker, P.F. (1982), The Cenozoic subduction history of the Pacific margin of the Antarctic Peninsula: ridge crest-trench interactions. *J Geol Soc London, 139*, 787-801.

Barrera, E. and S. M., Savin (1999), Evolution of late Campanian-Maastrichtian marine climates and oceans. In: Barrera, E. and Johnson, C.C. (Eds), Evolution of the Cretaceous Ocean-Climate System, Special Paper 332, *Geological Society of America*, 245-282.

Barron E.J. and W.H. Peterson (1991), The Cenozoic ocean circulation based on ocean General Circulation Model results, *Paleogeography, Paleoclimatology, Paleoecology, 83*, 1-28.

Berger, W.H., E. Vincent, and H.R. Thierstein (1981), The deep-sea record: major steps in Cenozoic ocean evolution. *In* Warme, J.E., Douglas, R.G., and Winterer, E.L. (Eds.), *The Deep Sea Drilling Project: A Decade of Progress*. Spec. Publ. Soc. Econ. Paleontol. Mineral, *32*,489-504.

Berggren W.A., D.V. Kent, C.C. Swisher III, M.-P. Aubry, (1995), A revised Cenozoic geochronology and chronostratigraphy, in: W.A. Berggren, D.V. Kent, M.-P. Aubry, J. Hardenbol, *Geochronology*, Time Scales and Global Stratigraphic Correlations: Framework for an Historical Geology, SEPM Spec,*54*, 129-212.

Bice, K.L., and J. Marotzke (2001), Numerical evidence against reversed thermohaline circulation in the warm Paleocene/Eocene ocean, J. *Geophys. Res., C, Oceans*, *106*, 11 – 15.

Boyle, E.A., (1981), Cadmium, zinc, copper, and barium in foraminiferal tests, *Earth and Planetary Science Letters*, *53*, 11-35.

Boyle, E. A., and L. D. Keigwin (1985), Comparison of Atlantic and Pacific paleochemical records for the last 215,000 years: changes in deep ocean circulation and chemical inventories, *Earth and Planetary Science Letters*, *76*, 135-150.

Bralower, T.J., and J., Mutterlose (1995), Calcareous nannofossil biostratigraphy of Site 865, Allison Guyot, central Pacific Ocean: a tropical paleogene reference section. *In* Winterer, E.L., Sager, W.W., Firth, J.V., and Sinton, J.M. (Eds.), *Proc. ODP, Sci. Results,* 143: College Station, TX (Ocean Drilling Program), 31–74.

Brass, G.W., J.R. Southam, W.H. Peterson (1982), Warm saline bottom water in the ancient ocean, *Nature, 296*, 620-623.

Broecker, W. S., R. Gerard, M. Ewing, and B. C. Heezen (1960), Natural radiocarbon in the Atlantic Ocean, *Geophy. Res., 65*, 2903-2931.

Chamberlin T.C., (1906), On a possible reversal of deep-sea circulation and its influence on geologic climates, *Proc. Am. Philos. Soc.* 33- 43.

Coachman, L., K. Aagaard, R. Tripp (1975), Bering Strait: the regional physical oceanography, *The University of Washington Press*, USA.

Daly, M., D. Smith, B. Hooper (1991), Cenozoic plate tectonics and basin evolution in Indonesia, *Marine and Petroleum Geology*, *8*, 2-21.

DePaolo, D. J., and G. J. Wasserburg (1976), Nd isotope variations and petrogenetic models, *Geophys. Res. Lett., 3,* 248-252.

Eagles, G., K. Gohl, and R. D. Larter (2004), High-resolution animated tectonic reconstruction of the South Pacific and West Antarctic Margin, *Geochem. Geophys. Geosyst., 5*, Q07002, doi:10.1029/2003GC000657.

Firth, J.V., (1995), Data report: Cenozoic calcareous nannofossils of Hole 869A, equatorial Pacific Ocean. *In* Winterer, E.L., Sager, W.W., Firth, J.V., and Sinton, J.M. (Eds.), *Proc. ODP, Sci. Results,* 143: College Station, TX (Ocean Drilling Program), 567–570.

Frakes, L. A. and E.L. Kemp (1972), Influence of continental positions on early Tertiary climates, *Nature, 240*, 97–100.

Friedrich, O., J. Erbacher, K. Moriya, P. Wilson, H. Kuhnert (2008), Warm saline intermediate waters in the Cretaceous tropical Atlantic Ocean, *Letters to Nature*, *1*, 453-457.

Goldstein, S. R. O'Nions, P. Hamilton (1984), A Sm-Nd isotope study of atmospheric dusts and particulates from major river systems, *Earth and Planetary Science Letters*, *70*, 221-236.

Goldstein, S.J., and S.B. Jacobsen (1987), The Nd and Sr isotopic systematic of river-water dissolved material: Implications for the sources of Nd and Sr in seawater, *Chem. Geol.: Isotope Geoscience Section*, *66*, 245-272.

Goldstein, S. J., and S. B. Jacobsen (1988), Nd and Sr isotopic systematics of river water suspended material – implications for crustal evolution, *Earth and Planetary Science Letters*, *87*, 249-265.

Hague, A., D. J. Thomas, M. Huber, R. Korty, S. Woodard, B. Jones (in review), Convection of North Pacific deep water during the early Eocene.

Hall, R., (2001), Cenozoic reconstructions of SE Asia and the SW Pacific: changing patterns of land and sea, *In Metcalfe, I, Smith, JMB, Morwood, M&Davidson, ID Faunal and Floral Migrations and Evolution in SE Asia-Australasia AA Balkema* (Swets & Zeitlinger Publishers) Lisse, 35-56.

Hall, R., (2002), Cenozoic geological and plate tectonic evolution of SE Asia and the SW Pacific: computer-based reconstructions, model and animations, *Journal of Asian Earth Sciences*, *20*, 353-431.

Hay, W.W., S. Flögel, E. Söding (2005), Is the initiation of glaciation on Antarctica related to a change in the structure of the ocean? *Global and Planetary Change*, *45*, 23-33.

Hollis, C., L. Handley, E. Crouch, H. Morgans, J. Baker, J. Creech, K. Collins, S. Gibbs, M. Huber, S. Schouten, J. Zachos, R. Pancost (2009), Tropical sea temperatures in the high-latitude South Pacific during the Eocene. *Geology*, *37*, 99-102.

Hollister, C., (1976), Proc. DSDP, Initial Reports, Site 323, Shipboard Scientific Party, *U.S. Government Printing Office*.

Hotinski, R. M., and J. R. Toggweiler (2003), Impact of a Tethyan circumglobal passage on ocean heat transport and ‘‘equable’’ climates, Paleoceanography, *18*, 1007- 1029.

Huber, M., and L.C. Sloan (2001), Heat transport, deep waters, and thermal gradients: 282 Coupled simulation of an Eocene greenhouse climate, *Geophysical Research Letters*, *283*, 3481-3484.

Jeandel, C., (1993), Concentration and isotopic composition of Nd in the South Atlantic Ocean, *Earth Planet. Sci. Lett. 117*, 581 – 591.

Jeandel, C., J. Bishop, A. Zindler (1995), Exchange of neodymium and its isotopes between seawater and small and large particles in the Sargasso Sea, *Geochimica et Cosmochimica Acta*, *59*, 535-547.

Jeandel, C., D. Thouron and M. Fieux (1998), Concentrations and isotopic composition of neodymium in the eastern Indian Ocean and Indonesian straits, *Geochimica et Cosmochimica Acta, 62*, 2597-2607.

Kerr, A.C., J.A. Aspden, J. Tarney, and L.F. Pilatasig (2002), The nature and provenance of ac- creted oceanic terranes in western Ecuador: Geochemical and tectonic constraints, *Geological Society [London] Journal*, *159*, p. 577–594.

Korty, R., K.A. Emanuel, and J.R. Scott (2008), Tropical cyclone-induced upper-ocean mixing and climate: application to equable climates, *Journal of Climate*, *21*, 638-654.

Lacan, F., and C. Jeandel (2005), Neodymium isotopes as a new tool for quantifying exchange fluxes at the continent-ocean interface, *Earth Planet. Sci. Lett.*, *232*, 245-257.

Larson, R., W. Pitman (1972), World-Wide correlation of Mesozoic magnetic anomalies, and its implications, *Geological Society of America Bulletin*, *83*, 3645-3662.

Lawver, L. A., and L. M. Gahagan (1998), Opening of Drake Passage and its impact on Cenozoic ocean circulation, in Tectonic Boundary Conditions for Climate Reconstructions, *Oxford Monogr. Geol. Geophys.*, *39*, edited by T. J. Crowley and K. C. Burke, 212 – 223, Oxford Univ. Press, New York.

Lawver, L. A., and L. M. Gahagan (2003), Evolution of Cenozoic seaways in the circum- Antarctic region, *Paleogeography. Paleoclimatoly, Paleoecology.*, *198*, 11–37.

Levitus, S. (1982), Climatological Atlas of the World Ocean, NOAA Prof. Pap. 13,173 , *U.S. Govt. Print. Off.*, Washington, D.C.

Ling, H. F., K. W. Burton, R. K. O'Nions, B. S. Kamber, F. von Blanckenburg, A. J. Gibb, and J. R. Hein (1997), Evolution of Nd and Pb isotopes in central Pacific seawater from Ferromanganese crusts, *Earth Planet. Sci. Lett., 146,* 1-12.

Ling, H. F., S.Y. Jiang, M. Frank, H.Y. Zhou, F. Zhou, Z. L. Lu, X. M. Chen, Y. H. Jiang and C.D. Ge (2005), Differing controls over the Cenozoic Pb and Nd isotope evolution of deepwater in the central North Pacific Ocean, *Earth Planet. Sci., Lett., 232,* 345-361.

Lyle, M., (1997), Could early Cenozoic thermohaline circulation have warmed the poles?,309 *Paleoceanography*, *12*, 161-167.

MacLeod, K., E. Martin, S. Blair (2008), Nd isotopic excursion across Cretaceous ocean anoxic event 2 (Cenomanian-Turonian) in the tropical North Atlantic, *Geology*, *36*, 811-814.

Martin, E. E., and B.A. Haley (2000), Fossil fish teeth as proxies for seawater Sr and Nd, *Geochim. Cosmochim. Acta, 64,* 835-847.

Martin, E.E., H.D. Scher (2004), Preservation of seawater Sr and Nd isotopes in fossil fish teeth: Bad news and good news, *Earth and Planetary Science Letters, 220*, 25-39.

Martin, E., S. Blair, G. Kamenov, H. Scher, E. Bourbon, C. Basak, and D. Newkirk (2010), Extraction of Nd isotopes from bulk deep sea sediments for paleoceanographic studies on Cenozoic time scales, *Chemical Geology*, *269*, 414-431.

Martin, H. A., (2006), Cenozoic climate change and the development of the arid vegetation in Australia, *Journal of Arid Environments*, *66*, 533-563

Mountain, G. S., and K.G. Miller (1992), Seismic and geologic evidence for late Paleocene - early Eocene deepwater circulation in the western North Atlantic, *Paleoceanography*, *7*, 423–439.

Murphy, D.P., and D.J. Thomas (2010), The negligible role of intermediate water circulation in stadial-interstadial oxygenation variations along the southern California margin: Evidence from Nd isotopes, *Quat. Sci. Rev., 29*, 2442-2450.

Najjar, R., G. Nong, D. Seidov, and W. Peterson (2002), Modeling geographic impacts on early Eocene ocean temperature, *Geophysical Research Letters*, *29*, 1750.

O'Nions, R. K., M. Frank, F. von Blanckenburg, and H.F. Ling (1998), Secular variation of Nd and Pb isotopes in ferromanganese crusts from the Atlantic, Indian, and Pacific oceans, *Earth Planet. Sci. Lett., 155*, 15–28.

Pagani, M., J. Zachos, K. Freeman, B. Tipple and S. Bohaty (2005), Marked decline in atmosphereic carbon dioxide concentrations during the Paleogene, *Science 309*, 600.

Pak, D. K., and K. G. Miller (1992), Paleocene to Eocene benthic foraminiferal isotopes and assemblages: Implications for deepwater circulation, *Paleoceanography*, *7*, 405–422.

Pearson, P.N., and M. R. Palmer (2000), Atmospheric carbon dioxide concentrations over the past 60 million years: *Nature*, *406*, 695–699.

Pettke,T., and A.N. Halliday (2002), Cenozoic evolution of Asian climate and sources of Pacific seawater Pb and Nd derived from eolian dust of sediment core LL44-GPC3, *Paleoceangraphy*, *17*,1031.

Person, A., H. Bocherens, J.F. Saliège, F. Paris, V. Zeitoun and M. Gérard (1995), Early Diagenetic Evolution of Bone Phosphate: An X-Ray-Diffractometry Analysis, *Journal of Archaeological Science, 22*, 211-221.

Piepgras, D.J., G.J. Wasserburg and E.J. Dasch (1979), Isotopic composition of Nd in different ocean masses, *Earth and Planetary Science Letters*, *45*, 223-236.

Piepgras, D.J., and G.J. Wasserburg (1982), Isotopic composition of neodymium in waters from the Drake Passage, *Science, 217*, 207-214.

Piepgras, D.J., and G.J Wasserburg (1987), Rare-Earth Element transport in the western North-Atlantic inferred from Nd isotopic observations, *Geochimica et Cosmochimica Acta, 51*, 1257-1271.

Piepgras, D.J., and S.B. Jacobsen (1988), The isotopic composition of neodymium in the North Pacific, *Geochimica et Cosmochimica Acta, 52*, 1373-1381.

Primeau, F., (2005), Characterizing transport between the surface mixed layer and the ocean interior with a forward and adjoint global ocean transport model, *American Meteorological Society*, *35*, 545-564.

Reynard, B., C. Lècuyer and P. Grandjean (1999), Crystal-chemical controls on rare-earth element concentrations in fossil biogenic apatites and implications for paleoenvironmental reconstructions, *Chem. Geol. 155*, 233-241.

Riley, T., P. Leat, R. Pankhurst, C. Harris (2001), Origins of Large Volume Rhyolitic volcanism in the Antarctic Peninsula and Patagonia by Crustal Melting, *Journal of Petrology*, *42*, 1043-1065.

Roberts, N.L., A.M. Piotrowski, J.F. McManus, and L.D. Keigwin (2010), Synchronous deglacial overturning and water mass source changes, *Science*, *327*, 75-78.

Rogl, F., (1976), Late Cretaceous to Pleistocene Foraminifera from the Southeast Pacific Basin, DSDP Leg 35, *DSDP, 35*, Initial Reports.

Sager, W.W., E.L. Winterer, J.V. Firth et al., Shipboard Scientific Party (1993), Introduction. *In Proc. ODP, Init. Repts.,* 143: College Station, TX (Ocean Drilling Program), 7–12.

Scher, H., E. Martin (2004), Circulation in the Southern Ocean during the Paleogene inferred from neodymium isotopes, *Earth and Planetary Science letters*, *228*, 391-405.

Shaw, H. F., and G. J. Wasserburg (1985), Sm-Nd in marine carbonates and phosphates, *Geochem. Cosmochim. Acta, 49,* 503-518.

Staudigel, H., P. Doyle, and A. Zindler (1985), Sr and Nd isotope systematics in fish teeth, *Earth Planet. Sci. Lett., 76*, 45-56.

Stickley, C. E., H. Brinkhuis, S. A. Schellenberg, A. Sluijs, U. Rohl, M. Fuller, M. Grauert, M. Huber, J. Warnaar, and G. L. Williams (2004), Timing and nature of the deepening of the Tasmanian Gateway, Paleoceanography, *19*, 1-18.

Storey BC, Alabaster T, Hole MJ, Pankhurst RJ, Wever HE (1992), Role of subduction-plate boundary forces during the initial stages of Gondwana break-up: evidence from the proto-Pacifc margin of Antarctica*, Geol Soc London Spec Publ 68*: 149-164.

Stott, L.D., J.P. Kennett, N.J. Shackleton and R.M. Corfield (1990), The evolution of Antarctic surface waters during the Paleogene: Inferences from the stable isotopic compositions of planktonic foraminifers, ODP Leg 113. In: Barker, P.F., J.P. Kennett, et al. *Proc. ODP, Sci. Results*, 113: College Station, TX (Ocean Drilling Program).

Tachikawa, K., C. Jeandel, and M. Roy-Barman (1999), A new approach to the Nd residence time in the ocean: role of atmospheric inputs, *Earth Planet. Sci. Lett., 170,* 433-446.

Talley, L. D., (1993), Distribution and formation of North Pacific intermediate water, *J. Phys. Oceanogr. 23*, 517–537.

Talley, L., (2003), Shallow, Intermediate and deep overturning components of the global heat budget, *J. Physical Oceanograph*, *33*, 530-560.

Taylor, S.R., and S.M. McLennan (1995), The geochemical evolution of the continental crust, *Rev. Geophys.*, *33*, 241-265.

Thiede, J., (1978), Proc. DSDP, Initial Reports, Site 463: Western Mid-Pacific Mountains, Shipboard Scientific Party, *U.S. Government Printing Office*.

Thomas, D. J., T. J. Bralower, and C. E. Jones (2003), Neodymium isotopic reconstruction of late Paleocene – early Eocene thermohaline circulation, *Earth Planet. Sci. Lett., 209*, 309 – 322.

Thomas, D. J., (2004), Evidence for production of North Pacific Deep Waters during the early Cenozoic greenhouse, *Nature, 430,* 65-68.

Thomas, D. J., M. Lyle, T. C. Moore Jr., and D. K. Rea (2008), Paleogene deepwater mass composition of the tropical Pacific and implications for thermohaline circulation in a greenhouse world, *Geochem. Geophys. Geosyst.*, *9*.

Tripati, A. K., M. L. Delaney, J. C. Zachos, L. D. Anderson, D. C. Kelly, and H. Elderfield (2003). Tropical sea-surface temperature reconstruction for the early Paleogene using Mg/Ca ratios of planktonic foraminifera, *Paleoceanography*, *18*,1101.

You, Y., (2003), The pathway and circulation of North Pacific Intermediate Water, *Geophysical Research Letters, 30*, No. 24, 2291.

Van de Flierdt, T., M. Frank, J. R. Hein, B Hattendorf, D. Gunther, and P. W Kubik, (2004), Deep and bottom water export from the Southern Ocean to the Pacific over the past 38 million years, *Paleooceanography*, *19*, 1020.

Winfrey, E. C., P.S. Doyle, and W. R. Riedel (1987), Preliminary ichthyolith biostratigraphy, southwest Pacific, *Deep Sea Drilling Project Leg 91, Initial Rep. Deep Sea Drilling Project*, *91*,447- 473.

Woodard, S.C., and D.J. Thomas (2009), Is it eolian dust? Contributions to the fine 373 silicate fraction of deep sea sediments on Shatsky Rise, 58 Ma, *Geochimica et 374 Cosmochimica Acta*, *73*, Supplemental Abstract A1452.

Woodard, S.C., D.J. Thomas, S. Hovan, U. Röhl, and T. Westerhold (2011), Evidence for orbital forcing of dust accumulation during the early Paleogene greenhouse, *Geochemistry Geophysics Geosystems*, *12*.

Wright, J., R. S. Seymour, and H. Shaw (1984), REE and Nd isotopes in conodont apatite: Variations with geological age and depositional environment, *Spec. Pap. Geol. Soc. Am., 196*, 325-340.

Zachos, J.C., L.D. Scott, and K.C. Lohnman (1994), Evolution of early Cenozoic marine temperatures, *Paleoceanography*, *9*, 353-387.

Zachos, J. C., M. Pagani, L. C. Sloan, E. Thomas, and K. Billups (2001), Trends, rhythms, and aberrations in global climate 65 Ma to present, *Science, 292*, 686-693.

Zachos, J.C., G.R. Dickens, and R.E. Zeebe (2008), An early Cenozoic perspective on greenhouse warming and carbon-cycle dynamics. *Nature. 451*, 279-283.

Zaier, A., A. Beji-Sassi, S. Sassi, and R. T. J. Moody (1998), Basin evolution and deposition during the Early Palegene in Tunisia, in *Petroleum Geology of North Africa*., edited by D. S. MacGregor, R. T. J. Moody and D. D. Clark-Lowes, 375- 393, Geological Society Special Publication, London.

Zhou, L., and F.T. Kyte (1992), Sedimentation history of the South Pacific pelagic clay province over the last 85 million years inferred from the geochemistry of Deep Sea Drilling Project Hole 596, *Paleoceanography*, *7*, 441-465.

APPENDIX A

SAMPLE PROCEDURE

I. *Sieving*

Bulk sediment samples were disaggregated in a dilute solution of sodium metaphospate solution before washing through a >63 micron (μm) sieve. Fish debris were then handpicked from washed samples.

II. *Cleaning*

A select few samples underwent an oxidative/reductive cleaning process marked as "cleaned" (C) and were compared with "uncleaned" (UC) fish debris.

The cleaned subset of samples initially underwent two sonicated rinses in ethanol followed by two sonicated rinses in ultrapure Milli-Q water. The samples were then processed through the oxidative/reductive cleaning process. For the oxidative step, 200 μl of 0.1 N NaOH and 30% hydrogen peroxide (H_2O_2) was added to each sample and placed in an 80˚C hot water bath for ten minutes. The oxidative solution was then aspirated off and samples were rinsed and sonicated with Milli-Q three times. For the reductive step, 100 μl of ammonium hydroxide (NH_4OH), citrate and hydrazine (NH_3NH_3) was added to each sample and placed in an 80˚C hot water bath for thirty minutes. The reductive liguid was then aspirated off and samples were rinsed and sonicated with Milli-Q three times. Finally, an acid leach made of 150 μl 0.001N HNO_3 was added on each sample and quickly pipetted off before being dissolved in 200 μl of 2N HNO_3.

Results verified that the Boyle cleaning [*Boyle, 1981; Boyle and Keigwin, 1985*] was not necessary and thus the remaining samples were processed in the unclean method using only two rinses in ethanol and in Milli-Q water before being dissolved in 200 μl of 2N HNO_3.

III. *RE Spec*

After removing the detrial material, samples were processed through RE Spec cation exchange chemistry to isolate the bulk REE suite from the bulk sample. RE Spec resin in Milli-Q was loaded into columns, cleaned twice with 3 mL of 0.05 N HNO_3 and then preconditioned with 3 mL of 2N HNO_3. Fish debris samples dissolved in 200 µl of 2N HNO_3, were then added to each column. A series of washes were then added to the columns including three 0.1 mL aliquots 2N HNO_3, two 0.5 mL aliquots of 2N HNO_3, and one 0.1 mL aliquot 2N HNO_3 and finally, one 1.5 mL aliquot 2N HNO_3. The REE were eluded with 4 mL of warm 0.05 N HNO_3 and then placed on a 65DC hot plate to evaporate and dry down as a nitrate. To prep for the next set of chemistry, samples were then converted to a chlorite by adding 50 µl of 1N HCL and 450 µl of Milli-Q for a total of 500 µl of 0.1N HCL.

IV. *Methyllactic Acid Chemistry*

Methyllactic acid chemistry was employed to chromatographically separate Nd from the rest of REE. BioRad resin in 0.15M (alpha)-HIBA acid was loaded into long glass columns. The resin was set with 200 µl of Milli-Q. Warmed samples in 500 µl of 0.1N HCL were then loaded into each column. Another 200 µl aliquot of Milli-Q was added to each column to set the sample. Samples were then washed with 10 mL and 10.75 mL batches of alpha-HIBA acid, 0.15, 5.5 mL and 5.75 mL of 0.225 alpha-HIBA acid, and then Nd was eluded with 3.25 mL of 0.225 alpha-HIBA acid. Collected samples were then placed on 65ºC hotplate to evaporate, with aqua regia to purge any remaining methylatic acid fibrous crystals.

V. *TIMS*

2N HCL was added to dried samples to load on a double rhenium (Re) filament, and then analyzed as Nd+ using the TIMS (Thermal Ionization Mass Spectrometer).

VI. *Leachate and Silicate Samples*

In addition a representative subset of samples were also analyzed for Nd isotopic composition of the detrital silicate fraction. For those samples, ~0.05g of powdered sample was added to a 50mL mixture 52/48 l M sodium acetate/ 1 M acetic acid and placed on a shaker table for an hour and a half to digest the carbonate in the samples. The samples were centrifuged down and the leachate was decanted off. Then Milli-Q was added to the solid residue, and vortexed to allow contact with all material, before being centrifuged down three times. Next, 14 mL of 0.02 M hydroxylamine hydrochloride (HH) in 20% acetic acid was added to each sample and placed on the shaker table for an hour and a half. The oxide leachate was decanted off of the samples, and used for analysis of seawater Nd on samples that did not have much fish debris. The leachate was centrifuged down for an hour, and poured into a beaker, leaving fines behind, and evaporated on a hotplate. The remaining solid residue was covered with 0.02 M HH in 20% acetic acid and placed on a shaker table for at least 24 hours. After decanting the HH solution, the samples were rinsed three times with Milli-Q and dried down. Samples were then powered and 0.2g of material was weighed out. The sample were then digested in 1 mL concentrated HNO_3 and 3.25 mL HF on a 100˚C hotplate for several days, until no particles were visible. The leachate and silicate samples when underwent RE Spec cation exchange chemistry and methyllactic acid chemistry as described before for the fish debris samples.

APPENDIX B

Nd isotope data generated in this study. "C" denotes Cleaned, "UC" denotes Uncleaned, "L" denotes Leachate, "D" denotes Detrital.

Hole 323							
Sample	**Depth (mbsf)**	**Age (Ma)**	**$^{143}Nd/^{144}Nd$**	**Abs error**	**eNd**	**Error**	**Met-hod**
14-2, 50-52	638.00	23.4	0.512281	0.000002	-6.4	0.04	UC
14-2, 60-62	638.10	23.5	0.512282	0.000004	-6.3	0.08	UC
14-2, 107-109	638.57	24.3	0.512304	0.000003	-5.9	0.05	UC
14-2, 121-123	638.71	24.5	0.512309	0.000009	-5.8	0.18	UC
14-2, 141-143	638.91	24.9	0.512304	0.000003	-5.9	0.06	UC
15-1, 121-123	656.46	53.2	0.512296	0.000002	-5.3	0.03	UC
15-2, 64-66	657.39	54.7	0.512301	0.000008	-5.2	0.15	UC
15-2, 109-111	657.84	55.4	0.512308	0.000003	-5.0	0.06	UC
15-3, 39-41	658.64	56.7	0.512289	0.000019	-5.4	0.37	UC
15-3, 115-117	659.40	57.9	0.512292	0.000002	-5.3	0.04	UC
15-4, 11-13	659.86	58.6	0.512287	0.000003	-5.4	0.05	UC
15-4, 39-41	660.14	59.1	0.512291	0.000002	-5.3	0.03	UC
15-4, 66-68	660.41	59.5	0.512275	0.000001	-5.6	0.03	UC
14-2, 141-143	638.91	24.9	0.512304	0.000003	-5.9	0.07	C
15-1, 121-123	656.46	53.2	0.512296	0.000003	-5.3	0.05	C
15-3, 39-41	658.64	56.7	0.512307	0.000003	-5.0	0.06	C
14-2, 141-143	638.91	24.9	0.512302	0.000002	-5.9	0.04	L
15-4, 66-68	660.41	59.5	0.512312	0.000002	-4.9	0.04	L
14-2, 141-143	638.91	24.9	0.512421	0.000001	-3.6	0.02	D
15-2, 64-66	657.39	54.7	0.512382	0.000003	-3.6	0.05	D
15-3, 115-117	659.40	57.9	0.512364	0.000002	-3.9	0.05	D
15-4, 66-68	660.41	59.5	0.512355	0.000002	-4.0	0.04	D
Hole 463							
6-3, 41-43	41.41	30.5	0.512386	0.000007	-4.1	0.13	UC
6-3, 95-97	41.95	30.6	0.512348	0.000005	-4.9	0.11	UC
6-3, 125-127	42.25	30.7	0.512393	0.000005	-4.0	0.11	UC
6-4, 8-10	42.58	30.7	0.512273	0.000004	-6.4	0.07	UC
6-4, 148-150	43.98	31.1	0.512404	0.000006	-3.8	0.12	UC
7-2, 26-28	45.26	50.1	0.512380	0.000002	-3.8	0.04	UC
7-2, 55-57	45.55	50.2	0.512382	0.000005	-3.7	0.09	UC
7-2, 93-95	45.93	50.3	0.512373	0.000004	-3.9	0.08	UC

7-2, 102-104	46.02	50.3	0.512378	0.000004	-3.8	0.08	UC
7-2, 123-125	46.23	50.4	0.512375	0.000005	-3.9	0.09	UC
7-2, 127-129	46.27	50.4	0.512366	0.000004	-4.0	0.08	UC
7-3, 11-13	46.61	50.5	0.512380	0.000003	-3.8	0.06	UC
7-3, 44-46	46.94	67.8	0.512301	0.000003	-4.9	0.06	UC
7-3, 115-117	47.65	67.9	0.512289	0.000001	-5.1	0.03	UC
7-3, 134-136	47.84	67.9	0.512302	0.000005	-4.9	0.10	UC
7-3, 115-117	47.65	67.9	0.512295	0.000006	-5.0	0.11	C
6-3, 41-43	41.41	30.5	0.512392	0.000002	-4.0	0.03	L
6-4, 8-10	42.58	30.7	0.512403	0.000002	-3.8	0.03	L
6-4, 148-150	43.98	31.1	0.512397	0.000001	-3.9	0.02	L
7-2, 55-57	45.55	50.2	0.512379	0.000002	-3.8	0.03	L
7-3, 44-46	46.94	67.8	0.512301	0.000001	-4.9	0.02	L
7-3, 44-46	46.94	67.8	0.511927	0.000009	-12.2	0.17	D
Hole 596							
3-2, 14-16	16.74	50.9	0.512310	0.000002	-5.1	0.03	UC
3-2, 53-55	17.13	53.0	0.512295	0.000002	-5.4	0.04	UC
3-2, 103-105	17.63	55.5	0.512266	0.000004	-5.9	0.07	UC
3-2, 132-134	17.92	57.0	0.512380	0.000002	-3.6	0.03	UC
3-2, 141-143	18.01	57.4	0.512276	0.000001	-5.6	0.02	UC
3-3, 31-33	18.41	59.4	0.512257	0.000002	-5.9	0.03	UC
3-3, 43-45	18.53	60.0	0.512259	0.000002	-5.9	0.04	UC
3-3, 63-65	18.73	60.9	0.512253	0.000001	-6.0	0.02	UC
3-3, 114-116	19.24	63.0	0.512274	0.000002	-5.5	0.04	UC
3-3, 137-139	19.47	63.8	0.512252	0.000003	-5.9	0.07	UC
3-4, 38-40	19.98	65.9	0.512258	0.000001	-5.8	0.02	UC
3-4, 77-79	20.37	67.4	0.512270	0.000002	-5.5	0.04	UC
3-4, 123-125	20.83	69.4	0.512272	0.000003	-5.4	0.05	UC
3-5, 27-29	21.37	71.7	0.512246	0.000004	-5.8	0.07	UC
3-5, 134-136	22.44	75.6	0.512237	0.000004	-5.9	0.08	UC
3-6, 22-24	22.82	77.8	0.512275	0.000002	-5.1	0.03	UC
3-6, 123-125	23.83	82.4	0.512252	0.000007	-5.5	0.14	UC
3-2, 141-143	18.01	57.4	0.512267	0.000004	-5.8	0.09	C
3-2, 14-16	16.74	50.9	0.512306	0.000002	-5.2	0.03	L
3-4, 77-79	20.37	67.4	0.512274	0.000004	-5.4	0.08	L
3-2, 14-16	16.74	50.9	0.512219	0.000001	-6.9	0.02	D
3-3, 31-33	18.41	59.4	0.512124	0.000001	-8.5	0.03	D

3-3, 114-116	19.24	63.0	0.512097	0.000002	-9.0	0.03	D
3-4, 77-79	20.37	67.4	0.512136	0.000002	-8.1	0.03	D
Hole 865B							
3-1, 15-17	18.15	31.8	0.512370	0.000003	-4.4	0.06	UC
3-1, 45-47	18.45	33.1	0.512367	0.000002	-4.5	0.04	UC
3-1, 110-112	19.10	36.1	0.512365	0.000002	-4.4	0.04	UC
3-1, 140-142	19.40	37.1	0.512360	0.000003	-4.5	0.05	UC
3-3, 56-58	21.56	37.8	0.512367	0.000004	-4.3	0.07	UC
4-2, 91-93	29.91	40.4	0.512386	0.000003	-3.9	0.06	UC
4-5, 37-39	33.87	41.2	0.512405	0.000006	-3.5	0.11	UC
4-5, 132-134	34.82	41.4	0.512410	0.000002	-3.4	0.05	UC
5-2, 67-69	39.17	42.2	0.512421	0.000005	-3.2	0.10	UC
6-3, 107-109	50.57	44.0	0.512422	0.000007	-3.1	0.13	UC
6-6, 82-84	54.82	44.5	0.512339	0.000097	-4.7	1.89	UC
7-3, 88-90	59.88	45.1	0.512379	0.000006	-3.9	0.11	UC
7-5, 72-74	62.72	45.5	0.512380	0.000005	-3.9	0.09	UC
8-2, 67-69	67.67	46.0	0.512408	0.000010	-3.3	0.19	UC
8-2, 114-116	68.14	46.2	0.512388	0.000004	-3.7	0.07	UC
8-6, 81-83	73.81	47.9	0.512356	0.000003	-4.3	0.06	UC
9-5, 111-113	82.11	51.1	0.512357	0.000007	-4.2	0.13	UC
9-6, 64-66	83.14	51.4	0.512352	0.000004	-4.3	0.08	UC
11-5, 55-57	100.55	54.6	0.512324	0.000007	-4.8	0.14	UC
11-6, 38-40	101.88	54.7	0.512325	0.000006	-4.7	0.11	UC
11-6, 71-73	102.21	54.8	0.512324	0.000002	-4.8	0.04	UC
12-4, 98-100	108.98	55.4	0.512351	0.000004	-4.2	0.09	UC
12-5, 134-136	110.84	55.6	0.512350	0.000005	-4.2	0.09	UC
13-3, 63-65	116.63	56.2	0.512353	0.000003	-4.1	0.07	UC
13-5, 68-70	119.68	56.6	0.512362	0.000002	-4.0	0.04	UC
14-4, 83-85	127.83	58.2	0.512332	0.000006	-4.5	0.11	UC
15-2, 15-17	133.65	60.2	0.512335	0.000004	-4.4	0.07	UC
15-2, 82-84	134.32	60.4	0.512344	0.000002	-4.2	0.04	UC
3-1, 140-142	19.40	37.1	0.512363	0.000002	-4.4	0.04	L
12-4, 98-100	108.98	55.4	0.512350	0.000002	-4.2	0.03	L
13-3, 63-65	116.63	56.2	0.512363	0.000002	-3.9	0.04	L
Hole 869A							
10-2, 45-47	87.65	37.0	0.512377	0.000002	-4.2	0.04	UC
10-2, 91-93	88.11	37.1	0.512359	0.000003	-4.5	0.06	UC
11-4, 59-61	100.59	41.5	0.512365	0.000002	-4.3	0.05	UC
12-3, 98-100	109.48	43.7	0.512344	0.000013	-4.6	0.26	UC
14-3, 100-102	129.50	45.2	0.512361	0.000010	-4.3	0.20	UC

10-2, 91-93	88.11	37.0	0.512361	0.000002	-4.5	0.04	C
10-2, 45-47	87.65	37.0	0.512356	0.000003	-4.6	0.05	L
15-3, 9-11	138.59	45.8	0.512319	0.000002	-5.1	0.04	L
15-3, 9-11	138.59	45.8	0.512319	0.000002	-5.1	0.04	L
10-2, 45-47	87.65	37.0	0.512281	0.000004	-6.0	0.07	D

VITA

Jessica Anna Schubert received her Bachelor of Science degree in Geology from The University of Texas at Austin in 2009. She entered the Geological Section of the Oceanography Department at Texas A&M University in January 2010 and received her Master of Science degree in May 2012. She may be reached at: Department of Oceanography, Texas A&M University, 3146 TAMU, College Station, TX 77843-3146.